Deltares
Enabling Delta Life
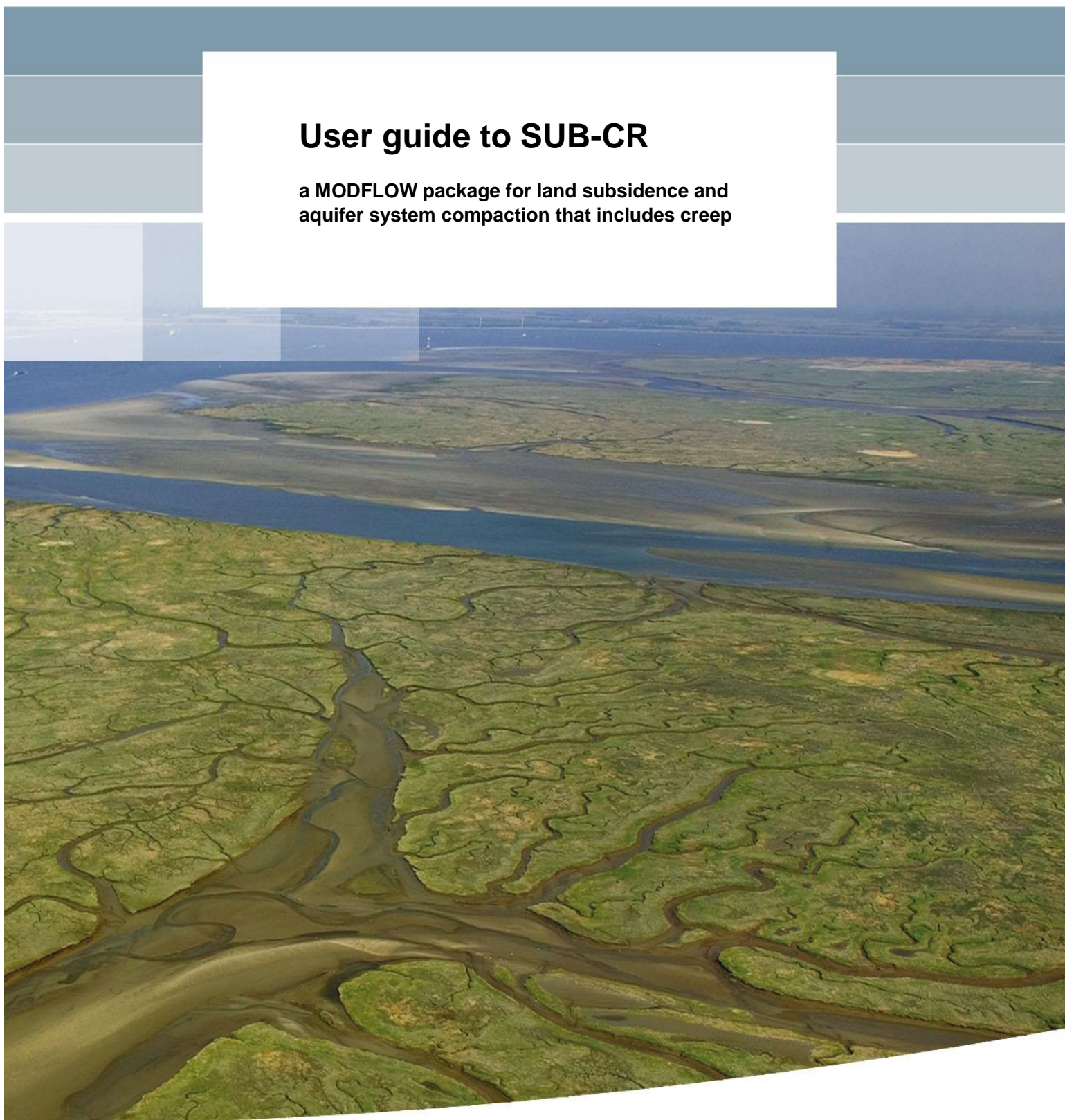
User guide to SUB-CR

a MODFLOW package for land subsidence and aquifer system compaction that includes creep

User guide to SUB-CR

a MODFLOW package for land subsidence and aquifer system compaction that includes creep

Henk Kooi
Mahmoud Bakr
Ger de Lange
Evert den Haan
Gilles Erkens

11202275-008

Title
User guide to SUB-CR

Client	Project	Reference	Pages
Deltares	11202275-008	11202275-008-BGS-0003	51

Keywords
MODFLOW, land subsidence, NEN-Bjerrum, abc, isotache, creep

Summary
This document is the user guide of SUB-CR, version 1.0. SUB-CR is a MODFLOW-2005 based land subsidence package developed by Deltares[1] that includes consolidation by creep. The package was developed to allow the modelling of land subsidence with a more comprehensive and more complete process representation of soft-sediment deformation than existing regional-scale hydrogeological models of land subsidence which do not consider creep. Creep and secondary consolidation are important in geotechnical applications involving soft-sediment (silt, clay, peat) consolidation. There is no obvious reason why creep would be irrelevant or insignificant when these sediments consolidate and cause land subsidence driven by groundwater use and groundwater management.

The guide provides (1) theoretical background of creep in soft-sediment consolidation, (2) a comprehensive description of the SUB-CR model formulation, including a derivation of model equations and discussion of assumptions, (3) practical information on package use in the form of input instructions and general modelling advice, and (4) results of (1-dimensional) example calculations that illustrate how creep affects subsidence behavior and that benchmark SUB-CR with a geotechnical code (viz. DSettlement) for settlement calculation that implements the same compression model(s).

Similar to the SUB-WT land subsidence package of MODFLOW, SUB-CR simulates compaction of interbeds (lenses or thin compressible layers within aquifers) or of extensive confining units, together with the associated compaction-driven flow, accounting for temporal and spatial variability of both geostatic and effective stresses. The calculated compaction response consists of an elastic and a viscous component (i.e. creep), with a choice between two constitutive relationships (NEN-Bjerrum and abc-isotache) that are used in codes for simulating settlement due to surface loads (viz. DSettlement). The NEN-Bjerrum method uses linear strain and parameters that are commonly determined in consolidation tests. The abc-isotache model uses natural strain, is considered more accurate for large strain, and uses parameters that are less widely reported in geotechnical tests, but that can be readily estimated from consolidation test parameters. The conventional Terzaghi-type elastoplastic constitutive behavior of existing MODFLOW land subsidence packages (IBS, SUB, SUB-WT) arises as a limiting case of the creep model when the coefficient of secondary compression is chosen very small. Similar to SUB-WT, geostatic stress can be treated as a function of water-table elevation. However, geostatic stress, pore pressure and effective stress are evaluated as averages for a model cell rather than local values for the bottom of a model cell.

An important implication of creep as implemented in SUB-CR is that considerably larger preconsolidation stresses tend to be required than in models or approaches without creep to produce similar amounts of irreversible (inelastic) compression of soft-sediments. Independent (field/laboratory) evaluation of preconsolidation conditions, therefore, should provide crucial information to judge the validity of either approach.

---

[1] The package is not part of the modules distributed by the USGS and the sole responsibility of Deltares.
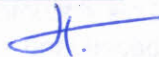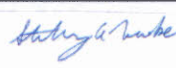
Deltares

Title
User guide to SUB-CR

Client	Project	Reference	Pages
Deltares	11202275-008	11202275-008-BGS-0003	51

Version	Date	Author	Initials	Review	Initials	Approval	Initials
	Aug. 2018	Henk Kooi	*K*	Gualbert Oude Essink	*B*	Henriette Otter	*H.*
		Mahmoud Bakr		Stan Leake (USGS)	*Stanley A. Leake*		
		Ger de Lange					
		Evert den Haan					
		Gilles Erkens					

State
final

Title
User guide to SUB-CR

Client	Project	Reference	Pages
Deltares	11202275-008	11202275-008-BGS-0003	51

Definition of basic terms

The following descriptions are meant to clarify the meaning of basic terms <u>in this guide</u>.

Subsidence
Lowering of the vertical position of a point at or below the ground surface relative to a defined datum.

Focus of the present guide is subsidence caused by vertical compression of the ground caused by groundwater extraction. The datum may then be considered to be the vertical position of any deep point below the depth interval in the ground that is subject to compression. On page B-4 subsidence is used in a broader sense, including subsidence by, for instance, deep-seated tectonic causes.

Land subsidence
The same meaning as subsidence. However, it commonly refers to subsidence of the land surface. Interpretation depends on context.

Settlement
Subsidence caused by the weight (load) of an artificial structure (building, embankment, road). Settlement of the ground surface in this context refers to the original ground surface because construction itself can entail an elevation of the ground surface (e.g. for embankments). In geotechnical engineering, settlement can also refer to the vertical movement of the structure itself. If the structure is rigid, and without foundation, its settlement equals that of the original land surface.

Compression
The process of reduction of the height of a parcel of ground/soil related to the state of (vertical) effective stress experienced by the parcel. Compression refers to a mechanical process. In this guide, creep is also considered to give rise to compression, even though an increase in effective stress need not be involved.
Negative compression in this guide is referred to as expansion or swelling.

Compaction
The process in which the soil matrix becomes more dense (compact) at the expense of pore space. In this guide the term is virtually identical to compression. The difference is that it is detached from (or less strongly tied to) considerations of stress conditions. The term compaction also is detached from considerations of rates of dewatering that are essential to the term consolidation.

Consolidation
Temporal development of the compression or compaction of a relatively low permeability layer, interbed, or test sample after a 'loading' event. Loading can either refer to application of a weight, or to reduction of the pore pressure near the top and/or bottom of the layer. During primary consolidation, the temporal development is limited by the rate at which pore

water can drain to the top and/or bottom of the layer. During secondary consolidation, the rate of compression of the soil matrix by creep dictates the rate of dewatering of the layer and the compression. The term consolidation is commonly used in soil mechanics.

Title
User guide to SUB-CR

Client	**Project**	**Reference**	**Pages**
Deltares	11202275-008	11202275-008-BGS-0003	51

List of Key Symbols

Symbol[2]	Unit	Description
$\dot{\$}$	$(\$) \cdot s^{-1}$	Time rate of change of variable $\$$
$\langle \$ \rangle$	$(\$)$	Vertical average of variable $\$$
Parameters of compression models		
a	-	Recompression or swelling index (abc-method)
b	-	Compression index (abc-method)
c	-	Secondary compression index (abc-method)
RR	-	Recompression or swelling ratio (NEN Bjerrum-method)
CR	-	Compression ratio (NEN Bjerrum-method)
C_α	-	Secondary compression ratio (NEN Bjerrum-method)
C_r	-	Recompression or swelling constant
C_c	-	Compression constant
$C_{\alpha e}$	-	Secondary compression constant
Coordinates and time		
x	m	Horizontal coordinate (Eulerian reference frame)
ξ	m	Horizontal material coordinate (Lagrangian reference frame)
y	m	Horizontal coordinate (Eulerian reference frame)
ψ	m	Horizontal material coordinate (Lagrangian reference frame)
z	m	Vertical coordinate (Eulerian reference frame)
ζ	m	Vertical material coordinate (Lagrangian reference frame)
t	s	Time
Other		
m	m	Layer or sample thickness
e	-	Void ratio (or base of natural log)
v	-	Specific volume
γ	$kg \cdot m^{-2} \cdot s^{-2}$	Specific weight
γ_w	$kg \cdot m^{-2} \cdot s^{-2}$	Specific weight of pore water
γ_s	$kg \cdot m^{-2} \cdot s^{-2}$	Saturated specific weight

---

[2] *Additional sub- and/or superscripts are explained in the text*

Deltares

Title
User guide to SUB-CR

Client	**Project**	**Reference**	**Pages**
Deltares	11202275-008	11202275-008-BGS-0003	51

Symbol	**Unit**	**Description**
γ_m	$kg \cdot m^{-2} \cdot s^{-2}$	Unsaturated (moist) specific weight
p	$kg \cdot m^{-1} \cdot s^{-2}$	Pore pressure
h	m	Hydraulic head
σ	$kg \cdot m^{-1} \cdot s^{-2}$	Total or geostatic stress (vertical component)
σ'	$kg \cdot m^{-1} \cdot s^{-2}$	(Terzaghi's) effective stress (vertical component)
σ_p'	$kg \cdot m^{-1} \cdot s^{-2}$	Preconsolidation stress (vertical component)
OCR	-	Overconsolidation ratio
ε	-	Strain (vertical component; default: linear strain)
ε^H	-	Natural strain (vertical component)
ε_e	-	Elastic component of strain
ε_{cr}	-	Creep component of strain
ε_{pl}	-	Plastic component of strain
τ	s	Intrinsic time
τ_{ref}	s	Intrinsic time of the reference isotache (default: 1 day)
K_{xx} or K_x	$m \cdot s^{-1}$	Horizontal component of the hydraulic conductivity tensor
K_{yy} or K_y	$m \cdot s^{-1}$	Horizontal component of the hydraulic conductivity tensor
K_{zz} or K_z	$m \cdot s^{-1}$	Vertical component of the hydraulic conductivity tensor
S_s	m^{-1}	Specific storage
S_{ske}	m^{-1}	Elastic (skeletal) specific storage
S_{skp}	m^{-1}	Plastic (skeletal) specific storage
W	s^{-1}	Conventional sources in the MODFLOW mass balance equation
Q	s^{-1}	Unconventional sources in the MODFLOW mass balance equation
Q_{creep}	s^{-1}	Source term due to creep in the MODFLOW mass balance equation

Contents

1 Introduction

1.1 Rationale

Exploitation of groundwater resources in sedimentary aquifer systems is known to be a prime cause of land subsidence in many parts of the world already for more than half a century (Poland and Davis, 1969). In particular where the magnitude and lateral extent of pore pressure decline becomes large after prolonged periods of groundwater extraction, a significant fraction of the pumped water can be released from storage in compressible (inter)beds and confining units (Poland et al., 1975; Galloway and Burbey, 2011; Gambolati and Teatini, 2015). Subsidence rates of decimeters per year have been recorded in several regions with accumulated subsidence in the course of decades totaling up to 9 m (Galloway and Burbey, 2011). The subsidence has become a factor that hinders or threatens socio-economic development in many areas around the world. In particular in densely populated coastal and deltaic regions, subsidence poses severe problems with increased incidence, depth, and duration of marine and riverine flooding, and damage to buildings and infrastructure through differential movements (Syvitski et al., 2009; Giosan et al., 2014; Schiermeier, 2014; Erkens et al., 2015; Schmidt, 2015; Galloway et al., 2016). It is expected that land subsidence will continue to be an important concern, notably in countries where reliance on groundwater as a resource remains high (e.g., Bakr, 2015).

Mathematical models of the groundwater flow and compaction processes are important tools in the activities needed to address land subsidence. These models not only support or test our level of understanding of the problem, but are also needed to make subsidence projections and to assist with the design and the assessment of the effectiveness of mitigating measures. Broad consensus exists about appropriate formulations for the modeling of groundwater flow. However, constitutive relationships for the deformation of the porous framework through which the water flows are less unique and depend, amongst others, on soil (sediment) lithology, temperature and pressure conditions, and to some extent also on scale.

The currently existing MODFLOW family of land subsidence packages of the United States Geological Survey (USGS) (IBS (Leake, 1990; Leake and Prudic, 1991), SUB (Hoffman et al., 2003), SUB-WT (Leake and Galloway, 2007)) is the most well-known and probably the most widely used set of tools for the simulation of land subsidence associated with groundwater flow in extensive aquifer systems. These packages differ in various respects (e.g. the treatment of the delayed response of compressible interbeds upon head changes in aquifer sediments or the treatment of the impacts of water table changes). However, they all deploy an elastoplastic stress-strain relationship to calculate compaction and subsidence. This approach is based on Terzaghi's poroelastic compression model developed in the mid 1920's.

By contrast, geotechnical engineering codes that are used in calculation of subsidence of buildings, embankments or other artificial constructs due to the extra weight these structures impose on underlying strata[3], mostly use more comprehensive compression models for 'soft-sediment' (e.g., peat and clay (NNI, 2012)) that include viscous deformation. These models and codes account for secondary compression or creep. At present, there is no clear answer to the question why creep would play an important role in soft-soil engineering, and, at the same time, be irrelevant or insignificant in land subsidence caused by groundwater

---

[3] *In engineering this subsidence is commonly referred to as settlement*

exploitation. Both applications involve compression of clays and peat that should share the same material behavior irrespective the cause of compression. We, therefore, are of the opinion that there is a need for practicable land subsidence software that includes creep.

This report presents SUB-CR, a new MODFLOW-2005 land subsidence package which allows choice between two constitutive relationships (NEN-Bjerrum and abc-isotache) that are used in geotechnical practice in The Netherlands for simulating compression due to surface loads. These compression models basically are generalizations of Terzaghi's elastoplastic compression model that is used in the existing MODFLOW land subsidence packages IBS, SUB, SUB-WT. A coefficient of secondary compression controls the extent to which the behavior deviates from elastoplastic behavior. Elastoplastic behavior can be modelled by setting this coefficient to zero.

1.2 Aim and structure of this guide

This guide is meant to clarify the concepts, theory and methods of SUB-CR, and to provide essential practical information for package use. Chapter 2 introduces the reader to the background of creep in soft-sediment consolidation. Chapter 3 presents the model formulation, both conceptually and in terms of the underlying physics and mathematics. Derivations of essential model equations and aspects of numerical integration are provided in the appendices. Chapter 4 addresses practical issues of model input and gives advice on model use. And finally, chapter 5 includes (1-dimensional) example calculations and benchmarking.

1.3 Required prior knowledge and advice for studying this guide

Meaningful use of the package SUB-CR is not trivial and requires considerable investment to familiarize oneself with the underlying theory and the practical aspects of proper model design, parameter value assignment, detection of potential causes of calculation problems, and interpretation of results. Readers of this guide are expected to have a fair understanding of (a) the classical groundwater theory and the associated parameters that are employed by MODFLOW, and (b) basic soil mechanics concepts, principles and jargon. Comprehensive knowledge of SUB-WT land subsidence package of the USGS is very useful, but is not a prerequisite. An effort was made to clarify concepts and terminology as much as possible in this document.

First users of this guide are recommended to start by reading *Definition of Basic Terms* in the first pages of this report. Apparently simple terms such as *subsidence*, *settlement*, *consolidation*, *compression* and *compaction* may be understood very differently by those interested in the SUB-CR package depending on their background. To avoid misunderstanding and frustration, the meaning of those terms as used in this guide, are elucidated in *Definition of Basic Terms*.

2 Background of creep in soft-sediment compaction

When soils are loaded, for instance by the weight of a newly constructed embankment that bears down on the underlying soil layers, the layers will compress. The associated reduction of the vertical thickness of the layers causes subsidence of the original land surface and settlement of the embankment. In general, the compression of the layers is not limited to the time the load is applied, but occurs over a prolonged period of time following the loading. The main reason for this delayed response is that compression of a saturated soil layer can only proceed at the rate at which pore water is expelled from the layer. In particular for thick low-permeability layers, this expulsion is slow. Pore pressures (and hence hydraulic head) are raised in the layer when the load is applied – the deviation from the non-loaded condition is called 'excess pressure'. Over time, the excess pressures return back to zero (they dissipate), and the water expulsion and associated compression slow down. Coeval with the declining pore pressure, effective stress[4] increases. In engineering, this time-dependent process of compression or compaction in which water expulsion and excess pore pressure decline play a central role, is called consolidation, or more specific: primary consolidation (Figure 2.1).

However, for certain soils compression continues after dissipation of excess pore pressure (e.g., Mesri, 1973; Leroueil and Hight, 2003; Olsson, 2010). This behavior, which is also seen in laboratory tests, is generally known as 'secondary consolidation' (Figure 2.1). Secondary consolidation signals that compression also occurs at constant effective stress. It indicates a viscous (e.g., Neuzil, 2003) skeletal response. This viscous behavior, not necessary limited to the phase of secondary consolidation, is referred to as creep. Creep has been observed and studied in the laboratory and in the field for clay and peat soils for about eight decades. Measurement of creep parameters is a standard practice in oedometer and constant-rate-of-strain laboratory tests (International Organization for Standardization, 2004).
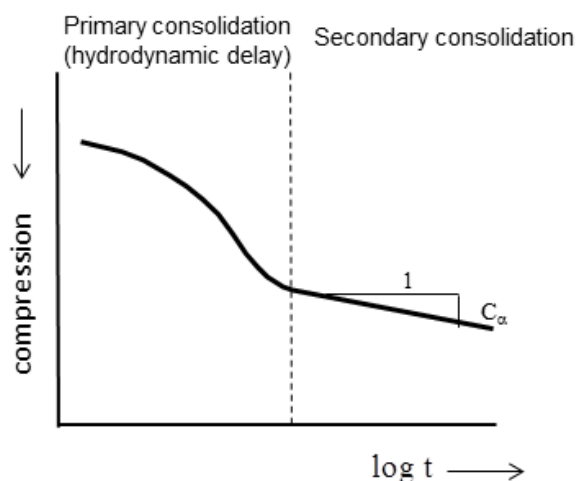
Figure 2.1   Phenomenological expression of creep in the form of secondary consolidation. Time is time since loading. The typical log-lin compression during secondary consolidation is commonly used to define a coefficient of secondary compression, C_α. Secondary compression cannot be represented through elastoplastic constitutive relationships.

---

[4] *The difference between the total ground stress and the pore pressure. Effective stress is a more fundamental quantity to describe deformation than pore pressure and total ground stress alone.*

Buisman (1936) was among the first to provide a mathematical expression for creep. He defined creep strain to increase proportionally with the logarithm of time after loading, and added it to the 'direct' component of deformation due to increase of (effective) stress. At about the same time, Gray (1936) represented creep as a "secondary time effect", where the period of primary compression coincides with Terzaghi's (1925) hydrodynamic increase of effective stress during drainage, and the viscous strain occurs during the subsequent period of secondary compression. Although Gray's approach had some practical advantages, the assumption that viscous strain (creep) does not impact the primary stage of consolidation was abandoned in later models (including the ones implemented in SUB-CR) and has recently been shown to be fundamentally flawed (Degago et al., 2013).

Taylor and Merchant (1940) proposed that, due to creep, there should be a family of stress-strain curves rather than a single curve describing the relationship between stress and strain. Each of these curves corresponds to a different duration of the applied load in a standard oedometer test. The curves were therefore called "time lines" (i.e. isochrones) (Figure 2.2a).
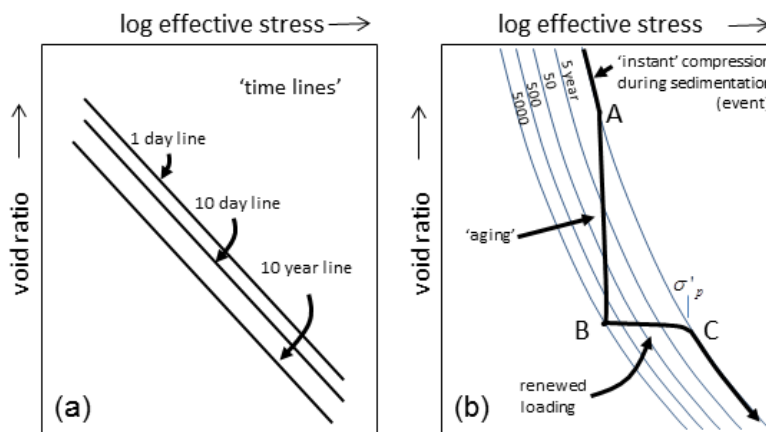

Figure 2.2 Different use of timelines in stress-strain diagrams. (a) Representing 'duration of loading' as proposed by Taylor (1942). (b) The time lines interpreted as 'isotaches', each with an 'intrinsic time'. The thick line denotes a path through stress-strain space illustrating 'aging' by creep (A-B), and an apparent overconsolidation response caused by subsequent loading (path B-C). Note the 'resetting' of intrinsic time to low values by the loading, reflecting a shift to high creep rates as proposed by Bjerrum (1967).

Curves for larger times (longer duration loading) correspond to larger strains (lower void ratio) and are 'shifted downwards' in the classical stress-strain graph.

These concepts were subsequently extended by Šuklje (1957) and Bjerrum (1967). Rather than lines of equal time, Šuklje (1957) proposed the use of isotaches, which are lines of equal rate of creep strain. Isotaches that plot lower in the (effective) stress – strain graph, or in the (effective) stress - void ratio graph, correspond to lower creep rates. Bjerrum (1967) subsequently combined the constant time and isotache concepts and assigned an 'equivalent time' to each rate of strain. Inspired by Szavits-Nossan (1988), Den Haan (1994a,b) finally renamed 'equivalent time' *intrinsic time*, and elaborated its relationship with creep rate based on work by Janbu (1960).

Creep rate is therefore now the fundamental quantity that is uniquely determined by void ratio (or strain) and effective stress, and *intrinsic time* is an indirect, or alternative measure of creep rate. An important advantage of this view is that the time measure (intrinsic time) has become detached from the too restrictive meaning of 'time since the start of loading'. Figure 2.2b shows that this idea was already exploited by Bjerrum who recognized that due to creep, 'aging' is associated with a progressive increase of apparent preconsolidation stress (yield stress), and that renewed loading 'resets' the equivalent (intrinsic) time to lower values, reflecting a shift to higher creep rates. This framework provided an elegant explanation of the apparent preconsolidation stress commonly observed in clays that experienced a regular burial history (normal consolidation). Where in elastoplastic approaches, preconsolidation stress could only be explained by unloading after a prior phase of higher effective stress, in this 'new' isotache-framework, the (apparent) preconsolidation stress can be due to creep, unloading, or a combination of both.

The isotache approach in soft-sediment deformation calculations – that is, models that use a constitutive relation in which creep rate is uniquely determined by strain and effective stress - has been adopted amongst others by geotechnical institutes in Canada, The Netherlands, Norway and Japan (Leroueil, 2006). In the Netherlands, Den Haan (1994a; 1996) defined the a,b,c-isotache model (in this guide abbreviated to abc-model), which has been laid down in the national industrial code of practice (SBRCURnet, 2005). This model is based on natural strain rather than the more conventional linear strain (these concepts will be elucidated in paragraphs 3.4.1 and 3.4.1, respectively). A version using lineair strain, which is referred to as the NEN-Bjerrum model, was derived from the abc-model to maintain continuity with older and wider known concepts.

In parallel with the development of these isotache models that employ a set of compression parameters that can be measured in standardized laboratory tests, a few other studies have proposed other unifying theories (e.g., poroviscosity; Helm (1998)). However, these models have neither seen widespread acceptance nor use.

Although the macroscopic phenomenon of creep has been well established through empirical methods, a proper understanding of the microscopic processes that underlie this behavior is still lacking. Mitchell (1993, p. 318) suggests that "secondary compression (creep) involves sliding at interparticle contacts, expulsion of water from microfabric elements, and rearrangement of adsorbed water molecules and cations into different positions".

3 Formulation

3.1 Basic assumptions

SUB-CR has been developed to be used in conjunction with MODFLOW, which is specifically designed to allow simulation of groundwater systems over large spatial domains. Not surprisingly, the package includes a number of key assumptions and simplifications that address aspects of scale, that also underlie the existing land subsidence packages of MODFLOW:

- Influences of horizontal components of stress and strain are neglected.
- (Vertical) effective stress is determined from pore pressure and the vertical component of geostatic stress.
- The concept of interbeds is used (Figure 3.1; Leake, 1990). This means that the behavior of aquifer units that contain relatively thin compressible lenses and layers (interbeds) that are tedious to model explicitly can be approximated by considering the fractional thickness of these beds in a model layer. Influences of the specific distribution of the interbeds in the aquifer and their geometric features are neglected.
- Hydrodynamic delay of compaction of interbeds due to slow release of water to the non-interbed aquifer fraction is neglected. A separate time scale for the delayed response as described for the SUB package (Hoffman et al., 2003) has not been included. However, delays are modeled explicitly for layers that consist fully of compressible sediments (confining layers).
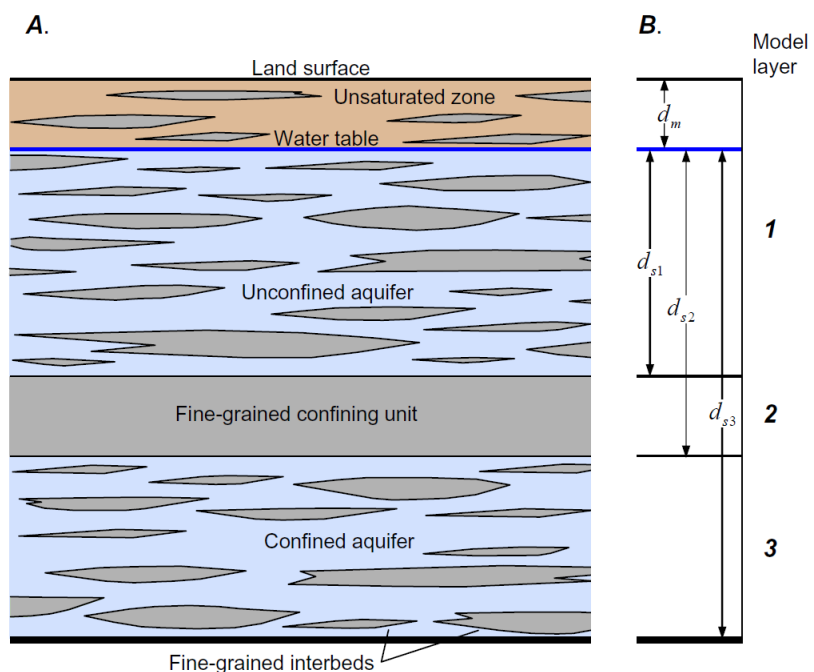- Subsidence due to compression of non-interbed materials is neglected.

Figure 3.1, Vertical section of a two-aquifer system with potential for compaction of fine-grained sediments. A, Hydrogeology of the system. B, Representation of the system with three model layers (Source: Leake and Galloway, 2007).

3.2 Basic features of the compression model

The right panel of Figure 3.2 illustrates the basic features of the viscoelastic compression model of SUB-CR in the form of a stress-strain diagram. The left panel depicts the equivalent Terzaghi-type elastoplastic compression model that is implemented in SUB-WT. The left panel has been included for the sake of reference to visualize commonalities and differences between the two models. Exhaustive, quantitative descriptions of the NEN-Bjerrum model and the abc-model are provided in sections 3.4.1 and 3.4.2, respectively.

The grey zones in both diagrams indicate stress-strain states that can be reached starting from the initial or reference state $\varepsilon = 0$; $\sigma' = \sigma'_o$. The only truly common feature of both models is that elastic strain accumulates when effective stress increases. This elastic strain is recovered upon subsequent reduction of effective stress. Differences exist in the way in which the accumulation of irreversible inelastic strain is described.

In the elastoplastic model, plastic strain accumulates in addition to the elastic strain when effective stress increases beyond the preconsolidation stress: $\sigma' > \sigma_p'$. This plastic strain develops instantaneously for a stress increase (ideal plastic behavior). For a monotonic increase of effective stress, stress-strain states follow the solid line that bounds the top of the grey zone. Ideal plasticity explains why stress-strain states above this line cannot occur in this model. Stress states below the elastic and the plastic bounding lines (indicated by the dark grey 'internal zone' in the graph) can only be reached when plastic strain has developed and effective stress is subsequently reduced.
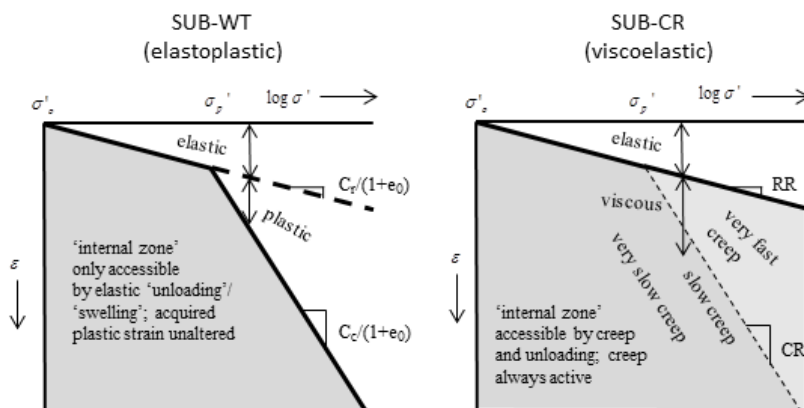
Figure 3.2, Illustration of basic features of the elastoplastic compression model of SUB-WT and the viscoelastic compression model of SUB-CR. σ', σ'_p and ε denote effective stress, preconsolidation stress, and strain, respectively. In SUB-CR viscous deformation (creep) is modeled throughout the grey zones. That is, the dashed line in the SUB-CR panel acts as a nominal (soft) boundary separating very fast from slow creep rates. States in the dark grey 'internal zone' can be established by creep, effective stress decrease (elastic unloading), or both. The compression parameters are elucidated in paragraph 3.4.

In the elastoplastic model, σ_p' increases with the effective stress when the effective stress increases beyond the prior preconsolidation stress level, and σ_p' remains unaltered when effective stress decreases. Therefore, by definition, σ_p' in this model equals the largest effective stress experienced by the sample. For any point in the diagram, the momentary σ_p' value can be inferred by drawing a line through the point that parallels the elastic bounding

line. The momentary σ_p' equals the effective stress for the intersection of that line with the plastic bounding line.

In the viscoelastic compression model of SUB-CR, viscous deformation (creep) accounts for the development of irreversible strain. A finite rate of strain (creep) is defined for all stress-strain states at and below the line that defines the elastic strain (also for $\sigma' < \sigma_p'$). This implies that when effective stress is kept constant, points tend to move downwards in the diagram as viscous strain accumulates. Above the dashed line – this line can be considered to be equivalent to the line that defines plastic strain in the elastoplastic model – creep rates are very fast. Therefore, when effective stress is constant, stress-strain states above the dashed line only exist for a very short time. Furthermore, a rapid increase of effective stress is needed to establish stress-strain states in this zone. Below and to the left of the dashed line creep rates decrease rapidly. Therefore, stress-strain states considerably below the dashed line can be reached in two ways: (1) by prolonged periods of creep; (2) by reduction of effective stress. A fundamental difference with the elastoplastic model is that in the viscoelastic model, effective stress does not have to exceed the preconsolidation stress for inelastic strain to accumulate.

In the viscoelastic model, the momentary σ_p' value is inferred in the same way from the diagram as in the elastoplastic model, where the value is read from the intersection with the dashed line that nominally separates fast and slow creep. Together with the viscous strain, this results in the following characteristics and behaviors that differ from the elastoplastic model and that are worth noting.

(1) For constant effective stress, creep causes σ_p' to increase with time. This follows from the fact that creep causes points to move downwards relative to the dashed line in the diagram.

(2) For constant effective stress the preconsolidation stress offset $\sigma_p' - \sigma'$ (commonly used to define overconsolidation) increases with time. This increasing degree of overconsolidation is also referred to as 'aging'. The preconsolidation stress offset, therefore, does not necessarily indicate an equivalent amount of 'unloading' has occurred.

(3) A simple relationship between σ_p' and the largest effective stress experienced by the sample does not exist.

(4) Although this requires exceptional conditions (a stress-strain state above the dashed line), an effective stress value that exceed the preconsolidation stress ('underconsolidation') can exist in the viscoelastic model.

3.3 Effective stress calculation

Effective stress, averaged over the depth interval of a model cell, is used in the compaction calculation. It is determined by differencing the average geostatic stress and the average pore pressure for the model cell.

$$\langle \sigma' \rangle = \langle \sigma \rangle - \langle p \rangle \tag{1}$$

Average geostatic stress is obtained from

$$\langle \sigma \rangle = \frac{1}{z_t - z_b} \int_{z_b}^{z_t} \sigma(z)dz \tag{2}$$

where z is positive upward, and where z_b and z_t denote the bottom and top position of the model cell. Geostatic stress as a function of vertical position is given by

$$\sigma(z) = \sigma_{surf} + \int_z^0 \gamma d\varsigma \tag{3}$$

where σ_{surf} represents a potential surface load and the integral is over bulk specific weight γ (solid phase plus pore fill). At present, similar to SUB and SUB-WT, globally constant values of bulk specific weight are used for saturated, γ_s, and for unsaturated (moist), γ_m, parts of the domain. And neither the vertical coordinates nor specific weight are corrected for compaction.

The average pore pressure of a model cell is determined from

$$\langle p \rangle = \gamma_w \left(\langle h \rangle - \langle z \rangle \right) \tag{4}$$

where h is head. In this expression average elevation, $\langle z \rangle$, corresponds to the middle of the model cell. Evaluation of average head for model cells that are partially or entirely unsaturated differs from that of saturated cells. For saturated cells, average head is given by the single head value, h_{cell}, provided through the finite difference scheme of MODFLOW

$$\langle h \rangle = h_{cell} \tag{5a}$$

For water table or dry cells

$$\langle h \rangle = h_{cell} + \tfrac{1}{2}\left(z_t - h_{cell}\right)^2 / \left(z_t - z_b\right) \tag{5b}$$

Equation (5b) assumes that hydraulic head in the unsaturated zone equals elevation head. This means that negative potentials associated with suction (capillary forces) are neglected.

In the SUB-CR code, the effective and geostatic stresses are normalized by the specific weight of (fresh) water such that their values correspond to equivalent heights of a water column. This facilitates comparison with values of hydraulic head.

Comparison with the method used in existing MODFLOW land subsidence packages

The use of cell-averaged estimates of effective stress in SUB-CR differs from approach adopted in the existing MODFLOW land subsidence packages IBS, SUB, SUB-WT. In the existing packages, effective stress is (nominally) evaluated for the base of model cells. Geostatic stress at the bottom of a model cell is based on equation (3). Pore pressure at the model cell base is determined using

$$p(z_b) = \gamma_w \left(h_{cell} - z_b \right) \tag{6}$$

An implicit assumption made here is that hydraulic head at the model cell base does not (significantly) differ from the cell-average hydraulic head. For this assumption to be valid, pore pressure should vary in the vertical according to a hydrostatic pressure gradient. Although this may be a reasonable approximation for cells with a high vertical hydraulic conductivity, it introduces a systematic bias in case of vertical flow through cells which represent (part of) a confining layer.

This bias does not compromise land subsidence calculations with the existing packages, because compression calculations in these packages are based on Terzaghi's poro-elastic compression model in which compression depends on effective stress change rather than effective stress. Changes in effective stress at the base of model cells appropriately represent cell-averaged changes in effective stress in the existing packages. An exception to this are water table model cells. However, in SUB-WT, the 'overestimated change of effective stress for such model cell as a whole' is compensated to a large extent by adjustment of the effective thickness of compressible sediments to sediments that are present below the water table only.

In SUB-CR, use of model cell-averaged values has been adopted instead of the existing approach for several reasons:

- It provides a more consistent method to relate initial effective stress to preconsolidation stress (and the associated overconsolidation ratio) and, thereby, to quantify the initial creep rate.
- The exact meaning of effective stresses reported in model output is directly comparable with reported heads (does not require the correction to model cell centre) and more in line with representative volume philosophy of finite difference models.
- The (effective) thickness of compressible sediments in model cells need not be head-dependent.
- It allows straightforward incorporation of the effective-stress-dependency of specific storage.

3.4 Strain calculation

Two models for the calculation of strain associated with the compression of sediments are implemented: the NEN-Bjerrum model and the abc-model (Den Haan, 1994a).

The NEN-Bjerrum model supports today's international standards for settlement prediction and is based on linear or Cauchy strain. The abc-model is a comparable model that employs natural or Hencky strain. The abc-model is included because it is superior for handling large strain and for cyclic change behavior of effective stress. However, this model is presently less well known and is primarily used by geotechnical engineers in The Netherlands.

3.4.1 The NEN-Bjerrum model

Linear strain

Linear strain is denoted here by ε. In the present context (1D), it represents the ratio of thickness change, Δm, and original thickness, m_o, of a layer that is subject to compression or swelling.

$$\varepsilon = \frac{\Delta m}{m_o} \tag{7}$$

In the continuum approach, m_o can itself be infinitesimally small. For convenience compression is adopted to represent positive strain. This implies that Δm is taken positive for a reduction of thickness.

Graphical representation of the compression model

The NEN-Bjerrum model decomposes total (linear) strain into two components, a direct elastic contribution ε_e and a time-dependent (secular) creep contribution ε_{cr}. Figure 3.3 depicts the essential features of the model. The left panel shows how the model defines a unique relationship among total strain ε (vertical axis), effective stress σ' (horizontal axis) and intrinsic time τ (red contour lines; also referred to as isotaches). Three compression parameters define the entire system: RR (recompression or swelling ratio), CR (compression ratio), and C_α (coefficient of secondary compression).
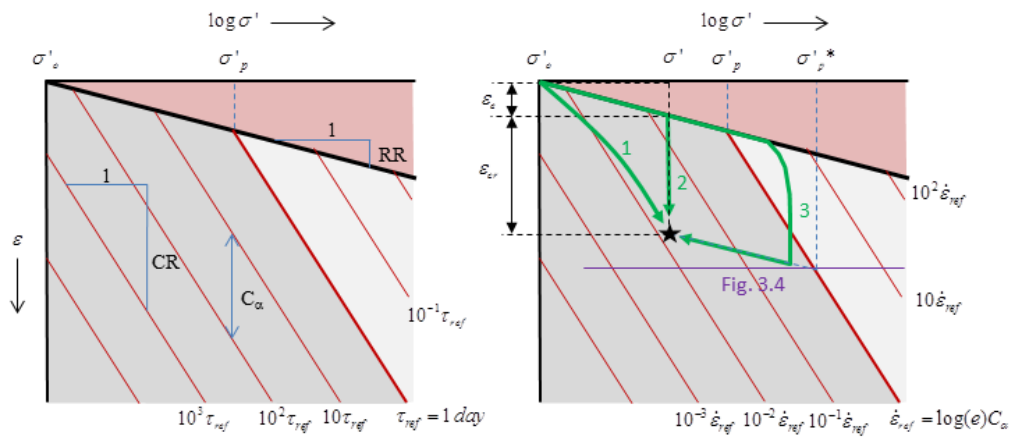

Figure 3.3, Graphical representation of the NEN-Bjerrum model. Isotaches are indicated by intrinsic time (left panel) and creep strain rate (right panel), where the subscript for creep strain in the strain rate has been left out to arrows) that are elucidated in the main text. 'log' represents the base 10 logarithm. The horizontal purple line in the right panel is a cross section in the diagram for which Figure 3.4 qualitatively illustrates how strain rate varies as a function of $\log \sigma'$. For reference, $\sigma'_p{}^*$ denotes the effective stress where the cross section crosses the reference strain rate ε_{ref} (or the reference isotache τ_{ref}). $\sigma'_p{}^*$ also equals the preconsolidation stress for the stress-strain state indicated by the star symbol in the diagram.

Intrinsic time and C_α define the creep strain rate through

$$\dot{\varepsilon}_{cr} = \frac{d\varepsilon_{cr}}{dt} = \frac{\log(e) \cdot C_\alpha}{\tau} \tag{8}$$

The right panel shows the contour map in terms of creep rate. The thick red contour, which corresponds to the $\tau = \tau_{\text{ref}} = 1\ day$ isotache, nominally separates stress-strain states associated with high creep strain rates (light grey zone) from states associated with low creep strain rates (dark grey zone)[5]. The actual transition from low to high creep rates across this 'boundary' is gradual and is controlled by C_α. This is schematically shown in Figure 3.4. For large C_α the transition is gradual and the creep rate at the 'boundary' is relatively high. For smaller C_α the transition is sharper, and the creep rate at the 'boundary' is less. The figure shows that, in the limit $C_\alpha \rightarrow 0$, the NEN-Bjerrum model approaches an elastoplastic rheology in which the light grey zone in Figure 3.3 represents a domain of direct 'virgin' compression (infinite creep rates = ideal plastic), while creep is absent in the dark zone. Under those circumstances, the reference isotache $\tau = \tau_{\text{ref}} = 1\ day$ defines an ideal 'yield' boundary, which is a fundamental feature of the classical poroelastic compression models, and plastic strain is basically a limiting case of creep strain.
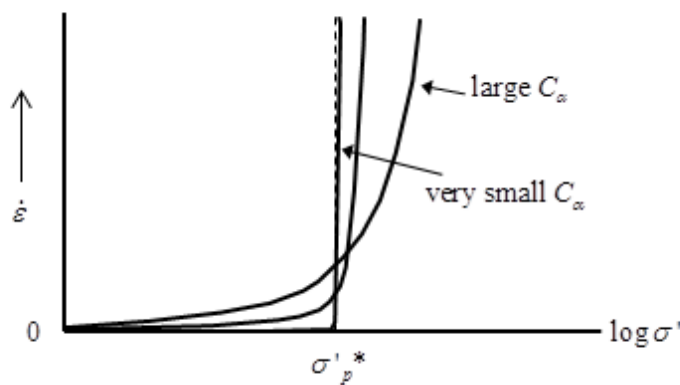

Figure 3.4, Schematic illustration of the way in which the coefficient of secondary compression controls the transition of creep rate across the 1 day reference isotache (cross section indicated in Figure 3.3). $\sigma'_p{}^*$ denotes the effective stress where the cross section crosses the reference strain rate ε_{ref} (or the reference isotache τ_{ref}).

In the graphs of Figure 3.3, σ'_o represents the effective stress corresponding to the zero-strain reference state. Note that this reference state will have a finite creep rate - for natural conditions in the subsurface this will be very small - determined by the intrinsic time associated with that state. The thick black line tracks the trajectory of elastic strain increase for a progressive increase in effective stress, and vice versa. The line, therefore, sets a minimum strain that is always present, and stress-strain states in the pink zone above this line can never be reached. In the course of time, and depending on the loading history, creep strain accumulates. This strain is considered irreversible (no negative creep rates) and augments the elastic strain. The right panel of Figure 3.3 shows an example of how total strain is decomposed in elastic and creep strain for the indicated stress-strain state (star). The green lines present a set of example pathways that could lead to that state. Path 1 reflects a fairly slow and progressive effective stress increase from σ'_o to σ'. It shows how creep strain can accumulate at effective stresses smaller than the preconsolidation stress

---

[5] *In this framework the term creep, therefore, is not restricted to strain in the dark grey zone; 'virgin compression in the light-grey zone is also established by creep (viscous deformation).*

given sufficient time. Path 2 indicates a virtually instantaneous increase to the final stress σ', followed by a period of creep without further stress change. Finally, path 3 represents a more complicated history. First an extremely rapid and large magnitude stress increase occurs in a very short time (fraction of a day) and is maintained for a few days. It shows that stress-strain states within the light grey (nominal 'plastic') zone can occur where creep rates are very high. The curved nature of the path arises because creep strain rates become very high and cannot be neglected during the short phase of effective stress increase. Then the effective stress is instantly reduced to the final value during which strain decreases by elastic rebound (or swelling).

As shown in Figure 3.3, in the NEN-Bjerrum model preconsolidation stress is directly coupled to the reference isotache $\tau = 1\ day$; σ_p' and $\sigma_p'^*$ respectively indicate the preconsolidation stresses for the initial (reference state), and for the example state indicated by the star in the right panel. The overconsolidation ratio for the example state, therefore, is $OCR = \sigma_p'^*/\sigma'$. A special feature of the model is that stresses larger than the preconsolidation stress ($OCR < 1$) can exist. For such conditions (position in the light grey zone in Figure 3.3), the creep strain rate is higher than that of the reference isotache. Isotaches not only indicate constant intrinsic time and constant strain rate, but also correspond to a constant OCR. That is, OCR, τ, and $\dot{\varepsilon}_{cr}$ are uniquely related via the three compression parameters RR, CR, and C_α (the expressions are provided in Appendix, and by e.g. Leoni et al. (2008)).

Mathematical representation of the compression model

The relationship between strain, stress and intrinsic time as depicted in the left panel of Figure 3.3 is fully described by the following expression[6]:

$$\varepsilon = RR \log\left(\frac{\sigma'_p}{\sigma'_o}\right) + CR \log\left(\frac{\sigma'}{\sigma'_p}\right) + C_\alpha \log\left(\frac{\tau}{\tau_{ref}}\right) \tag{9}$$

The separate elastic and creep strain components are given by:

$$\varepsilon_e = RR \log\left(\frac{\sigma'_p}{\sigma'_o}\right) + RR \log\left(\frac{\sigma'}{\sigma'_p}\right) = RR \log\left(\frac{\sigma'}{\sigma'_o}\right) \tag{10a}$$

$$\varepsilon_{cr} = (CR - RR) \log\left(\frac{\sigma'}{\sigma'_p}\right) + C_\alpha \log\left(\frac{\tau}{\tau_{ref}}\right) \tag{10b}$$

It is important to emphasize that the two terms on the right-hand side of Eq. (10b) together define the creep strain, because ε_{cr}, as given in Eq. (10b) develops through viscous deformation in the NEN-Bjerrum model. That is, creep strain is not limited to the second term. The latter interpretation may come naturally to those who recognize that the first term is identical to plastic strain in an elastoplastic deformation model employing RR and CR only.

---

[6] It should be noted that σ_p' in this expression represents the preconsolidation stress in the initial state, and is not updated when the momentary effective stress σ' exceeds this value.

The NEN-Bjerrum model is not a three-component elastic-plastic-creep model. This is borne out by the fact that the second term in Eq. (10b) can assume negative values – this corresponds to the light grey zone in Figure 3.3 – while the creep strain, fundamentally, can only result in positive strain (compression). Eq. (10b) does show that, in the limit $C_\alpha \to 0$, the NEN-Bjerrum model approaches an elastoplastic rheology.

After coupling with the groundwater flow model (paragraph 3.6), the strain needs to be updated for each model time step. The method of temporal integration for both the NEN-Bjerrum and abc-models is described in Appendix 7A.

3.4.2 The abc-model

Natural strain

Natural (or Hencky) strain is denoted by ε^H. Natural strain is based on the notion that the reference thickness for quantifying strain (m_o in linear strain) is itself changing during compression or swelling. With this concept, a 'more natural' measure of strain results

$$\varepsilon^H = \int_{b_o}^{b_{final}} \frac{1}{m} dm \tag{11a}$$

where m_o is the initial thickness, and m_{final} the final thickness of the layer. Natural strain relates to linear strain in the following way

$$\varepsilon^H = -\ln(1-\varepsilon) \tag{11b}$$

Use of natural strain has the advantage that the compression parameters obtained with this measure of strain remain applicable (constant) to high strain levels (compression levels). The abc-model exploits this advantage.

Graphical representation of the compression model

Figure 3.5 shows a graphical representation of the abc-model. Essential differences compared to the NEN-Bjerrum model (Figure 3.3) are:

- RR, CR and C_α are replaced by the reloading/swelling <u>constant</u> a, the compression <u>constant</u> b, and the secondary compression <u>constant</u> c. Below it is explained how both parameter sets are related.

- Natural (e-base) log of effective stress along the horizontal axis.

- Natural strain along the vertical axis.

- The vertical spacing between contours with a ten-fold change of intrinsic time or strain rate is $\ln(10)c$ (or spacing is c for an e-fold change).

- $$\dot{\varepsilon}^H = \frac{d\varepsilon^H}{dt} = \frac{c}{\tau} \tag{12}$$
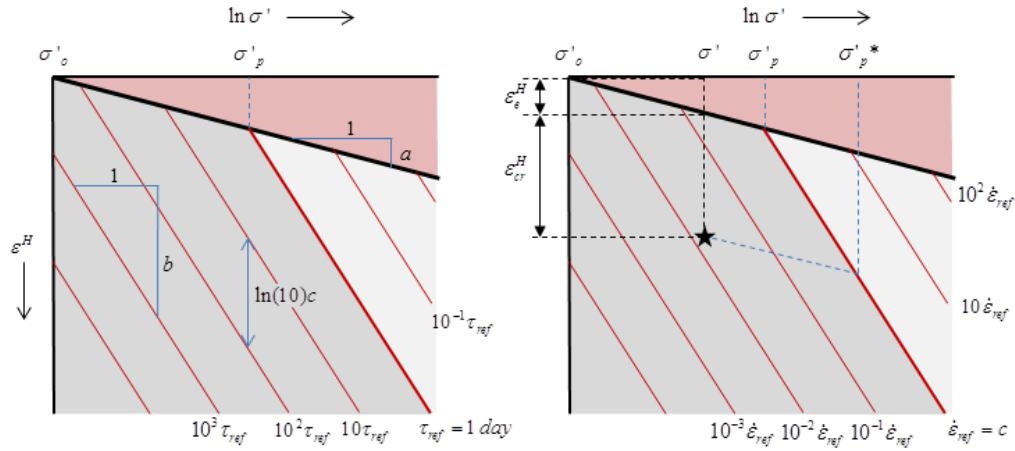
Figure 3.5, Graphical representation of the abc-model.

Mathematical representation of the compression model

The equations for total strain, direct strain and secular strain are:

$$\varepsilon^H = a \ln\left(\frac{\sigma'_p}{\sigma'_o}\right) + b \ln\left(\frac{\sigma'}{\sigma'_p}\right) + c \ln\left(\frac{\tau}{\tau_{ref}}\right) \tag{13}$$

$$\varepsilon_e^H = a \ln\left(\frac{\sigma'}{\sigma'_o}\right) \tag{14}$$

$$\varepsilon_{cr}^H = (b-a) \ln\left(\frac{\sigma'}{\sigma'_p}\right) + c \ln\left(\frac{\tau}{\tau_{ref}}\right) \tag{15}$$

3.5 Relationships among compression parameters

Table 3.1 summarizes the relationship among different compression parameters that are obtained in standard oedometer tests (International Organization for Standardization, 2004). Compression indices are included because they are commonly found in geotechnical test reports. Indices are derived from lin-log plots with void ratio along the compression axis. Because notations and naming conventions can differ, it is important to ascertain which compression axis quantity the parameter is associated with. In particular the notation of the coefficient of secondary compression can give rise to erroneous interpretation as the additional e in the subscript that indicates index rather than ratio is often left out.

Table 3.1   Relationships among compression coefficients

	Compression axis	Reloading/swelling	(virgin) compression	Secondary compression
Indices	Void ratio	C_r	C_c	$C_{\alpha e}$
Ratios	Linear strain	$RR = \dfrac{C_r}{1+e_o}$	$CR = \dfrac{C_c}{1+e_o}$	$C_\alpha = \dfrac{C_{\alpha e}}{1+e_o}$
Constants	Natural strain	$a = \dfrac{RR}{\ln(10)}$	$b = \dfrac{CR}{\ln(10)}$	$c = \dfrac{C_\alpha}{\ln(10)}$

To convert reported lab-test indices to ratios the original reference state (zero compression) void ratio e_0 of the test is needed. Ratios generally are constant over a larger range of compression than values of indices, which decrease together with void ratio. In SUB-CR indices (and constants), therefore, are true material constants and not updated based on momentary modelled void ratio as is done in SUB-WT.

For strain levels (up to ~ 0.05) the NEN-Bjerrum model and the abc-model are virtually indistinguishable. For those conditions, the conversion shown in Table 3.1 is very accurate.

3.6   Coupling of strain and groundwater flow

The partial differential equation that is solved through the coupling of SUB-CR and MODFLOW-2005, and which quantifies hydraulic head in space and time and, thereby, groundwater flow is:

$$S_{ske}\frac{Dh}{Dt} = \frac{\partial}{\partial x}\left(K_{xx}\frac{\partial h}{\partial x}\right) + \frac{\partial}{\partial y}\left(K_{yy}\frac{\partial h}{\partial y}\right) + \frac{\partial}{\partial \zeta}\left(K_{zz}\frac{\partial h}{\partial \zeta}\right) + W + Q_{creep} \tag{16}$$

D/Dt denotes the material derivative (relative to the moving solids). $\zeta = z(t = 0)$ indicates that calculations are performed on the initial undeformed grid. S_{ske} is the specific storage coefficient which accounts for the elastic deformation of the porous medium. W accounts for conventional sources such as wells and flux boundary conditions. Q_{creep} is a source term which represents the inelastic (creep) strain rate and quantified as follows.

$$Q_{creep} = \dot{\varepsilon}_{cr} = \frac{C_\alpha}{\ln(10)\tau} \quad \text{(NEN-Bjerrum model)} \tag{17a}$$

$$Q_{creep} = \dot{\varepsilon}_{cr}^{H} = \frac{c}{\tau} \quad \text{(abc-model)} \tag{17b}$$

For low values $C_\alpha < 10^{-4}$ and $c < 10^{-4}$, where creep rates are extremely sensitive to very small variations in effective stress near the 1-day isotache, and numerical solution is problematic due to strong non-linearity, Q_{creep} is quantified using a purely elastoplastic model. Non-zero values (when effective stress exceeds the preconsolidation stress of the previous time step) then are obtained using:

$$Q_{creep} = \dot{\varepsilon}_{pl} \approx \frac{S_{skp}}{\Delta t}\left[\frac{\sigma_n}{\gamma_w} - h_n + z - \frac{\sigma'_{p,n-1}}{\gamma_w}\right] \tag{18a}$$

$$S_{skp} \approx \frac{(CR - RR)\gamma_w}{\ln(10)\sigma'_n} \quad \text{(NEN-Bjerrum parameters)} \tag{18b}$$

$$S_{skp} = \frac{(b - a)\gamma_w}{\sigma'_n} \quad \text{(abc parameters)} \tag{18c}$$

where the subscript n indicates the time level, and where S_{skp} is a plastic specific storage coefficient.

For interbed cells/layers, the Q_{creep} values of Eqs (17 and 18) are multiplied by the 'interbed fraction', viz. the fractional thickness of the cell that consists of compressible interbeds. For partially saturated cells Q_{creep} is also multiplied by the saturation fraction of the cell, considering that the creep strain compresses (and dispels) the air phase in the unsaturated zone. The creep source contribution is listed as a separate term in the reported water balance. A derivation of Eqs (16) and (17) and the implicit assumptions that underlie it are provided in Appendix 7B.

Similar to SUB and SUB-WT, in the finite difference expression of Eq (16) the source term for the elastoplastic model (Eq 18a) is effectively moved to the left-hand side (separate additions to HCOF and RHS arrays of MODFLOW). This is possible due to the presence of h_n in linear form in Eq (18a). The approach is similar to the use of a plastic specific storage coefficient in addition to the elastic one rather than a source term. However, in the current approach the storage coefficient is internally calculated from the compression parameters and momentary effective stress and not specified. The same approach could be used for the elastic specific storage coefficient using the following relationships (Appendix 7B; e.g., Jorgensen, 1980).
.

$$S_{ske} = \gamma_w \frac{RR}{\ln(10)\sigma'} \quad \text{(NEN-Bjerrum model)} \tag{21a}$$

$$S_{ske} = \gamma_w \frac{a}{\sigma'} \quad \text{(abc-model)} \tag{21b}$$

However, in the present version 1.0 of SUB-CR the elastic specific storage coefficient is specified in the MODFLOW input files and not calculated internally.

The creep strain rate (Eq 17) cannot be represented in terms of a specific storage coefficient (viscous). Creep represents an *active* process that occurs irrespective of the effective stress conditions (constant, decreasing, increasing) and can only be handled as a true source term. For constant effective stress (nominally constant head), for instance, the porous medium is actively 'squeezed' by the creep. Elastic (or ideal plastic) compression, by contrast, is *passive* in the sense that it is slave to effective stress change (i.e., no effective stress change → no elastic strain).

Special measures to handle non-linearity

The head-dependency of the creep rate, and hence, of Q_{creep} (Eq 17), renders equation (16) non-linear. Non-linearity is particularly strong when the effective stress state approaches (or coincides with) the light grey zone in Figure 3.3 and Figure 3.5, for which conditions creep rates rapidly increase for a small reduction of hydraulic head. This non-linearity is handled by the outer iterations in MODFLOW. During package development and its testing, it was found that convergence tends to be slow (zigzag pattern with sequential overshooting/ undershooting) when Q_{creep} is directly based on the hydraulic head value inferred for an iteration. Moreover, overshooting can readily yield negative effective stress estimates during iteration for which no solution exists. To stabilize and speed up convergence the following adjustments were made: (1) SUB-CR returns a Q_{creep} -value to MODFLOW based on the average effective stress of the present and the previous iteration; (2) in case of negative effective stresses (unphysical state), a small effective stress-value is returned equal to 1% of the effective stress during the previous time step to allow continuation of the iteration process. If the solution truly requires negative effective stress, no convergence will be reached and the calculation prematurely stopped with a corresponding error message.

4 Input Instruction and general modeling advice

Input for the SUB-CR Package is read from the file that has the type "SCR" in the name file. The contents of the "SCR" file are described in 4.2. However, additional considerations are important to ensure successful use of the SUB-CR package and generation of meaningful models. These considerations are given here first.

4.1 Do's (and don'ts)

4.1.1 General

Model design and convergence testing

1. Include the entire subsurface volume explicitly. SUB-CR will give an error message in case of quasi-2D or quasi-3D models in which confining layers are represented by their resistance or leakance values. Thus, layers should be contiguous. This is required to be able to quantify geostatic stresses properly. Moreover, the temporal behavior of confining layers tends to play a crucial role in land subsidence and should be modeled explicitly.

2. For confining layers with an interbed fraction of 100%, specify input with a slightly smaller fraction (e.g. 99.9%)[7]. Calculations will be aborted if the thickness of compressible material (interbeds) exceeds the layer thickness. This can occur (be interpreted as such) if the thickness in the input file equals the layer thickness because of truncation errors of numbers.

3. Refine model layering to check for so-called 'grid convergence'. Representing a confining layer as a single model layer generally leads to a poor numerical approximation of the physical system that is modeled and bias in the calculated subsidence (see section 5.5 for a clear example). This is true for transient groundwater flow models in general. Good looking results are no indication of absence of bias. Also refine closure conditions (see 9).

4. Try to avoid large 'shocks' by changing boundary conditions or stresses (wells). Small time steps may be needed to handle the feedback of creep to pore pressure for model cells where imposed conditions force rapid pore pressure change. That is inherent to the physics of creep. If time steps are too large, the model will not converge and terminate prematurely. Time steps equal or less than one day are quite common. In general, it should be expected that much smaller time steps are required than those typically used in MODFLOW models that do not use SUB-CR. There are no guidelines yet to a-priori determine the maximum time steps that will ensure a completion of the run.

5. Refine time stepping to check for 'time-step convergence'. The implicit temporal integration scheme of MODFLOW-2005 allows the use of relatively large time steps, but results for the employed spatial discretization may still be inaccurate. This is true for transient groundwater flow models in general, but impacts calculated subsidence as well. Also refine closure conditions (see 9).

---

[7] *N.B.: model input is the thickness of compressible material for a model layer, not a fraction. Fractions are used in the code.*

6. In model design, avoid circumstances where head in the top layer can significantly exceed the layer top (land level), as this may result in negative effective stress levels. Such conditions should be regarded unphysical as the ground would burst creating a high-permeability zone with strong seepage. The negative effective stress indicates that the vertical permeability in the model or other aspects of model design are not appropriate. Such unphysical conditions go undetected in regular MODFLOW use, but for SUB-CR it is critical: it will not be able to calculate subsidence and terminate the run. A warning that negative effective stresses have been encountered in the calculations is given upon abortion. Mitigation options: a. modify boundary conditions or vertical permeability to lower head; b. increase the thickness of the top layer; c. increase specific weight (if reasonable); d. add a surface load (GL0), in particular at cells representing surface water, see next point.

7. If the top of the upper model layer represents a water bottom (river, lake, sea), special measures may be needed to avoid negative effective stress and premature ending of calculations. In the present SUB-CR version 1.0, the weight of the surface water column which is external to the model domain is not included in the geostatic stress. The weight of the overlying water can be added by specifying a surface load GL0. This is a model constant, therefore dynamic variations cannot be handled.

8. Modeling consolidation of sediments near or above the water table (for water table decline and /or rise) is difficult and non-trivial. Using a *confined layer type* for the top layer (for instance with a realistic specific yield value to handle storage) yields greatest numerical stability and virtually no convergence problems. However, the user should be aware that for such a choice unphysical conditions may arise, for instance when head (water table) becomes lower than the bottom of the cell. Under such conditions the nominally 'dry' cell remains active, delivering water to the underlying cell. A *convertible layer type* (set in the LPF package) yields more realistic results, but MODFLOW2005 often has problems achieving iterative convergence when the water table is close to the base of a cell, and a-priori setting appropriate convergence criteria is difficult. The same applies when *re-wetting* is used. Without re-wetting the convertible layer type tends to yield unphysical results when water table rises. Further work is still needed to look for practicable setting/approaches to use SUB-CR in models that include significant water table variations.

4.1.2 Parameterization

Convergence criteria / closure conditions

9. To obtain accurate results very tight closer conditions (notably of HCLOSE) for the solver packages must be used, often much tighter than those that may suffice for MODFLOW models that do not use SUB-CR. This is needed to force MODFLOW to use sufficient (outer) iterations to solve the feedback of creep to hydraulic head and flow properly. Most often the PCG solver package will be used. For special models, for instance when drying and wetting is used, the GMG solver package may be required (Wilson and Naff, 2004). Current experience indicates that HCLOSE=1.0E-4 or smaller is generally needed. Convergence testing – checking if the subsidence change is minimal for further reduction of HCLOSE – is a proper strategy to follow.

Compression parameter values

10. Paragraph 3.5 gives important information for conversion of laboratory test data to model parameter values. Care should be taken to carefully check the definition of the parameters in test reports or literature. Aspects of scale may have to be considered as well. Laboratory tests may be biased to relatively pure and fine grained core samples, while on a larger scale confining units may include coarser-grained interlayers.

11. Correlations between the three compression parameters can be useful to come up with a first set of values where some or all of the three parameters are missing (for example the secondary compression parameter). The table below lists typical ratios of secondary to virgin compression established by Mesri and Godlewski (1977).

Material	$C_{\alpha e} / C_c = C_\alpha / CR = c / b$
Granular soils, including rockfill	0.02 ± 0.01
Shale and mudstone	0.03 ± 0.01
Inorganic clays and silts	0.04 ± 0.01
Organic clays and silts	0.05 ± 0.01
Peat and muskeg	0.06 ± 0.01

12. Consider modelling coarse-grained aquifer units (without compressible interbeds) as 100% Interbed unit, albeit with compression properties for the coarse-grained sediment. Even when compressibility is small and creep negligible relative to fine grained material, the compression of very thick coarse grained aquifer units may still provide a relevant contribution to land subsidence and/or elastic rebound.

Preconsolidation stress

13. Use preconsolidation stresses that are consistent with creep and ageing. For existing land subsidence packages that are based on Terzaghi's elastoplastic compression model (SUB, SUB-WT), the preconsolidation stress is often estimated from ideas about the lowest hydraulic head in the past (e.g., Leake and Galloway, 2007). Preconsolidation stress is then assigned by specifying a constant increment above initial effective stress. However, this simple and pragmatic approach is inconsistent with creep. In creep-susceptible soft deposits (clay, peat) preconsolidation stress tends to increase by 'aging'. In particular in normally consolidated deposits, which have neither experienced large historic water table or head declines, nor recent large-magnitude unloading by erosion, preconsolidation stress should be expected to increase more strongly with depth than a constant increment above the present effective stress. Experience with SUB-CR indicates that use of a constant overconsolidation ratio $OCR = \sigma'_p / \sigma'$, is both very practicable and yields reasonable results. Minderhoud et al. (2017), for instance, recently inferred a constant OCR of 1.6 for clay units to several hundred meter depth from the modeling of the subsidence development of the Mekong delta, Vietnam. This OCR value is consistent with preconsolidation data of

geotechnical studies which report OCR ranging between 1.2 and 2.0. However, much more needs to be learned about actual preconsolidation stresses in various settings.

14. Make sure chosen overconsolidation ratio OCR values are sufficiently high to avoid unrealistically high initial – this usually represents prepumping conditions - creep strain rates. If the creep strain rate is too high, it will either cause excessive background subsidence for permeable strata that consolidate readily, or will cause a period in which hydraulic head rises strongly in thick confining layers until this increase is balanced by drainage. The latter increase happens because the initial, steady-state head profile for SUB-CR is obtained by solving a steady flow problem without creep. In the period needed to reach dynamic equilibrium, layer expansion can even cause net uplift. The following relationships determine the creep strain rate.

$$\dot{\varepsilon}_{cr} = \frac{d\varepsilon_{cr}}{dt} = \frac{\log(e) \cdot C_\alpha}{\tau} \qquad\qquad \tau = \tau_{ref} OCR^{\frac{CR-RR}{C_\alpha}}$$

$$\dot{\varepsilon}^H = \frac{d\varepsilon^H}{dt} = \frac{c}{\tau} \qquad\qquad \tau = \tau_{ref} OCR^{\frac{b-a}{c}}$$

Where τ_{ref} = *1 day*. These relationships can be readily used in a spreadsheet to determine creep rates for a proposed input, and for given layer thicknesses these can be used to estimate the corresponding subsidence for a depth profile.

Storage property values

15. Assign realistic S_{ske} values (e.g., Eqs. 21a,b). In the present version of the SUB-CR package, S_{ske} is a user-specified constant per cell/layer. This implies that is up to the user to come up with a set of mutually consistent parameter values for RR or a on the one hand (these are used in the strain and subsidence calculations) and elastic specific storage on the other, accounting as much as possible for the overall increase of effective stress with depth. For interbed cells this includes the effect (averaging) of potentially differing elastic properties of fine-grained (interbed) and course-grained sediments in the cell. Formally, S_{ske} should here include the storage effect of pore water compression. However, this storage generally is negligibly small (e.g., Gambolati and Freeze, 1973). Note that the required input values of specific storage for SUB-CR are different than for SUB or SUB-WT. For the latter packages, specific storage should account for pore water compressibility only (not indicated in the corresponding user manuals (Hoffmann et al., 2003; Leake and Galloway, 2007) because total strain, including the elastic component, is included in the source term.

16. Make sure the proper storage parameter is chosen. MODFLOW allows specification of storativities [non-dimensional]. These values implicitly include layer thickness (= product of specific storage and layer thickness). This implies that if model layers are refined, the storage value should be modified accordingly. Specific yield (storativity of a phreatic layer) should not be modified upon refining as it does not include layer thickness.

.

4.2 Sample SCR input file

The sample problem consists of 3 layers, one row and one column (see *discretization file* below). Two layers (layer 2 and 3) contain 'interbed systems'. Note that preconsolidation stress values (here OCR values) are specified for all model layers.

```
# SCR input file
36 1 2 0 2 2
2 3
constant 0.0000000E+00
constant 1.700000
constant 2.000000
constant 10.00000
constant 0.1000000
constant 0.3000000
constant 1.3000000E-02
constant 0.7500000
constant 0.0000000E+00
constant 1.000000
constant 2.0000001E-03
constant 4.0000002E-03
constant 0.0000000E+00
constant 0.7500000
constant 0.0000000E+00
constant 1.500000
constant 1.500000
constant 1.500000
-1 36 -1 36 -1 36 -1 36 -1 36 -1 36 -1 36 -1 36
1 10 1 1 1 1 1 1 1 1 1 1 1 1 1 1 1 1 1 1
```

```
# Discretization file
3 1 1 10 4 2 tbcheck
0 0 0
constant 10.00000
constant 10.00000
constant 0.0000000E+00
constant -1.000000
constant -11.00000
constant -12.00000
0.0000000E+00 1 1.000000 SS
4.000000 1 1.000000 TR
6.000000 1 1.000000 TR
10.00000 1 1.000000 TR
10.00000 1 1.000000 TR
10.00000 1 1.000000 TR
10.00000 1 1.000000 TR
25.00000 2 1.000000 TR
25.00000 2 1.000000 TR
50.00000 4 1.000000 TR
```

4.3 SCR file content description

Input Instructions

Note: all stress inputs in equivalent water column height

Data Set 0   [#Text]
                                    Item 0 is optional; "#" must be in column 1. Item 0 can be repeated
                                    multiple times.

Data Set 1   ISCRCB ISCROC NSYSTM NOBSSUB IMETHOD ISPCS

    ISCRCB is a flag and unit number.
        If ISCRCB > 0, it is the unit number to which cell-by-cell flow terms will be written when
        "SAVE BUDGET" or a non-zero value for ICBCFL is specified in MODFLOW Output
        Control (for example, Harbaugh and others, 2000, p. 52– 55).
        If ISCRCB ≤ 0, cell-by-cell flow terms will not be recorded.

    ISCROC is a flag and unit number.
        If ISCROC > 0, it is the number of repetitions of item 15 to be read, each repetition of which
        defines a set of times steps and associated flags for printing and saving subsidence-related
        info.
        If ISCROC ≤ 0, subsidence-related info will not be printed or saved.

    NSYSTM is the number of systems of interbeds (also those with 100% compressible sediments).

    NOBSSUB is the number of observation points to extract relevant results at specific cells
        (all systems of interbeds for a given row, column).

    IMETHOD is a flag to select the compression model. 1 = abc-model; 2 = NEN-Bjerrum model.

    ISTPCS is a flag to determine how initial preconsolidation stress input is given: 0= full values,
        1=offset values, 2=OCR values

Data Set 2   LNWT(NSYSTM)

    LNWT is a one-dimensional array specifying the model layer assignments for each of the
        NSYSTM systems of interbeds.

Data Set 3   [IROWOBSSUB ICOLOBSSUB (NOBSSUB)] if NOBSSUB > 0

    IROWOBSSUB is the row index of observation cell for which relevant results should be extracted
    ICOLOBSSUB is the column index of observation cell for which relevant results should be extracted

Data Set 4   GL0(NCOL,NROW)

    GL0 is the geostatic stress at the top of model layer 1   [m]

Data Set 5   SGM

    SGM is the specific gravity of unsaturated sediments (relative to water)   [-]

Data Set 6   SGS

    SGS is the specific gravity of saturated sediments (relative to water)   [-]

FOR EACH INTERBED SYSTEM

Data Set 7   THICK(NCOL,NROW)

    THICK is the thickness of compressible sediments (interbeds)   [m]

Data Set 8   ISOARR(NCOL,NROW)

    ISOARR is RR (NEN-Bjerrum) or a (abc)   [-]

Data Set 9   ISOBCR(NCOL,NROW)

    ISOBCR is CR (NEN-Bjerrum) or b (abc)   [-]

Data Set 10   ISOCCA(NCOL,NROW)

    ISOCCA is C_α (NEN-Bjerrum) or c (abc)   [-]

Data Set 11   VOID(NCOL,NROW)

    VOID is the initial void ratio (only for tracking change, does not affect subsidence)   [-]

Data Set 12   SUB0(NCOL,NROW)

    SUB0 is the initial compaction (translates into an initial subsidence)   [m]

FOR EACH LAYER

Data Set 13   PCS(NCOL,NROW) or PCSOFF(NCOL,NROW) or OCR(NCOL,NROW)

PCS (ISTPCS=0)	Preconsolidation stress	[m]
PCSOFF (ISTPCS=1)	Preconsolidation stress offset	[m]
OCR (ISTPCS=2)	Overconsolidation ratio	[-]

GENERAL

Data Set 14   [Ifm1 Iun1 Ifm2 Iun2 Ifm3 Iun3 Ifm4 Iun4 Ifm5 Iun5 Ifm6 Iun6 Ifm7 Iun7 Ifm8 Iun8]
                         if ISCROC> 0

Ifm# is a code for the format in which output will be printed (explanation of # below item 15)
Ifu# is the unit number to which output will be written if saved on disk (explanation of # below item 15)

Data Set 15   [ISP1 ISP2 ITS1 ITS2 Iflp1 Ifls1 Iflp2 Ifls2 Iflp3 Ifls3 Iflp4 Ifls4 Iflp5 Ifls5 Iflp6 Ifls6
                         Iflp7 Ifls7 Iflp8 Ifls8] if ISCROC > 0.

                         ISCROC records of 20 integers

ISP1 is the starting stress period in the range of stress periods to which output flags Ifl1 through Ifl16 apply.
ISP2 is the ending stress period in the range of stress periods to which output apply.
ITS1 is the starting time step in the range of time steps in each of the stress periods ISP1 through ISP2.
ITS2 is the ending time step in the range of time steps in each of the stress periods ISP1 through ISP2.

Iflp# output flag for saving to an unformatted file for the set of time steps specified by ISP1, ISP2, ITS1, and ITS2.

Ifls# output flag for saving to a formatted file for the set of time steps specified by ISP1, ISP2, ITS1, and ITS2.

The meaning of flag numbers # of items 14 and 15 are:

(1) Subsidence (= vertical displacement) of the top of layers
(2) Compaction of layers
(3) Preconsolidation stress of layers
(4) Geostatic stress of layers
(5) Effective Stress of layers
(6) Void ratio of interbed system layers
(7) Interbed thickness of interbed system layers
(8) Intrinsic time of interbed system layers

5 Sample Simulations

In this chapter, sample simulations are presented that illustrate:

(1) how SUB-CR predictions compare with that of other software (benchmarking),
(2) differences in performance of the abc-model and NEN-Bjerrum model for large strains,
(3) creep versus ideal plastic ('no creep') behavior,
(4) the importance of appropriate discretization in SUB-CR models.

The simulations focus on the response of thick soft-sediment units as both creep and the coupling with groundwater flow are most pronounced for such layers. The illustrative sample simulations are fictitious in the sense that they do not represent a specific field case with observational data. The set of sample simulations is envisaged to be extended in future versions of the package this guide, for instance to provide examples for subsidence associated with interbed systems and effects of water table changes. The SCR input file presented in paragraph 4.2 provides the input for the most basic simulation included in the set of simulations discussed in this chapter.

5.1 D-SETTLEMENT and FlexPDE

The benchmarks in this section compare the subsidence calculated by SUB-CR with those calculated by D-SETTLEMENT (a software product of Deltares Software Systems dedicated to the settlement prediction for the design of earth embankments (Deltares, 2011)), and FlexPDE 6.1, a scripted generic finite element solver for partial differential equations (pdesolutions.com).

D-SETTLEMENT includes both the NEN-Bjerrum and the abc model. Although D-SETTLEMENT is designed to address the impacts of surface loads, subsidence induced by drawdown of head in aquifer units can be readily simulated through 'water loads'. The water load option in D-SETTLEMENT is the equivalent of a time-varying constant head boundary condition in MODFLOW where 'load' refers to a change relative to hydrostatic conditions. This allows a close comparison of settlement predictions for 1-dimensional vertical flow systems. The concept of interbed systems that include a mixed response behavior to imposed stresses is not available in D-SETTLEMENT. That is, in D-SETTLEMENT compressible beds have to be modeled explicitly. Consequently, in the benchmarks the response of a confining layer (100% interbed) is evaluated.

As an extra check to verify that SUB-CR and the way it is coupled to MODFLOW yields a proper solution of the set of model equations, the equations were also implemented in, and solved with, FlexPDE.

5.2 General description of the simulations

A simple three layer conceptual model was used for the code inter-comparison (Figure 5.1). Layers here refer to geological strata, not MODFLOW calculation layers. The top and bottom layers represent thin aquifer units; the middle layer a 10 m thick confining unit consisting of

low permeability compressible sediments (viz. clay). Hydraulic head in the top layer is kept fixed. This layer is assumed not to contribute to subsidence (not included as an interbed system in the input). Starting from an initial hydrostatic (no flow) condition, head in the bottom layer is instantly reduced (drawdown). This initiates downward flow and head reduction in the overlying confining layer and associated compression of this layer. Both the elastic response of the bottom layer and the compression of the confining layer cause subsidence. Both a small-strain case and a large-strain case are modelled by imposing a small and a large drawdown, respectively. The imposed drawdown for the large-strain case of 6 m may seem rather large, but is not unrealistic. Even larger long-term drawdowns of about 9 m associated with groundwater extraction below the ~ 10 m thick Holocene cover layer exist in The Netherlands and have induced widespread, albeit poorly documented.
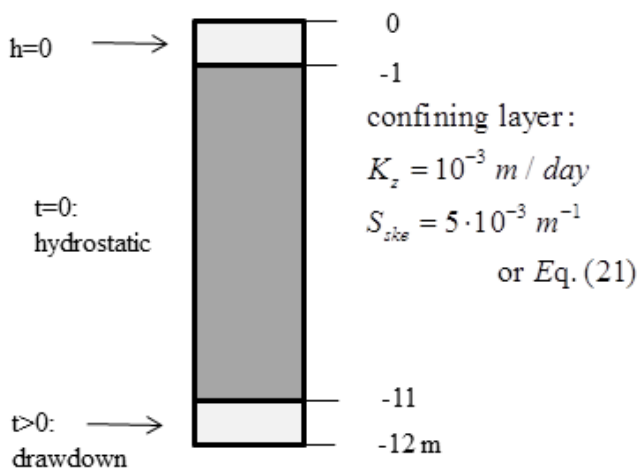

Figure 5.1, General characteristics of the sample simulations and benchmarks, in which the confining layer is stressed by an instantaneous drawdown of head in the bottom layer. A 'small-strain' (drawdown of 1 m) and a 'large-strain' (drawdown of 6 m) problem is solved.

Because the 'water load' function of D-SETTLEMENT used for the bottom layer assumes a hydrostatic pressure gradient (constant head) over the thickness of the layer to which a water load is applied, the hydraulic properties of the bottom (and top) layer in the SUB-CR and FlexPDE simulations were chosen accordingly (arbitrary very high vertical hydraulic conductivity and low specific storage). In SUB-CR a general head boundary condition, with very high conductance, is used to simulate the 'instantaneous' drawdown in the bottom layer. In FlexPDE, the head specified at the base of the bottom layer is lowered exponentially from the hydrostatic to the drawdown value with an e-folding timescale of 1 minute. D-SETTLEMENT and FlexPDE include built-in methods to ensure grid- and time step convergence. For SUB-CR, for the temporal discretization presented below, progressive finer discretization of the confining unit was used to test grid-convergence. Results are presented for converged simulations in which the confining layer is represented by 20 MODFLOW model layers. The specific gravity of saturated sediment was set to a constant value of 2 (an unsaturated zone does not develop in these sample simulations), which, in keeping with MODFLOW terminology, means that the saturated bulk density is 2 times that of pure water. This is an overestimate for clays at these shallow depths, but unimportant for illustrating the general model behavior and for model intercomparison presented below. Compression parameter values assigned to the two sediment types are listed in Table 5.1. Parameter values for the NEN-Bjerrum and abc-model were chosen to yield virtually identical results for small strain.

The chosen values are typical for soft clays and moderately dense sands of the Holocene deposits in the western part of The Netherlands (Table 2.b in NNI, 2012).

Table 5.1   Geo-mechanical properties used in the sample simulations

Layer type	RR [-]	CR [-]	C_α [-]	a [-]	b [-]	c [-]
Confined	0.100	0.300	0.013	0.04343	0.13029	0.00565
Aquifer	0.002	0.004	0.000	0.00087	0.00174	0.00000

Parameters that were varied among the various simulations are the overconsolidation ratio, the imposed drawdown in the bottom aquifer, and the simulated time (duration of the response).

5.3 Benchmark results

5.3.1 Small strain

Results for a problem with small strain are displayed in Figure 5.2. Results are presented for the NEN-Bjerrum model. The abc-model yields results (not shown) that are virtually identical. The fact that D-SETTLEMENT uses an effective stress dependent elastic specific storage (Eq. (21)) and FlexPDE and SUB-CR a constant elastic specific storage (Figure 5.1) explains small differences that occur in the first 50 days. The results for SUB-CR were obtained for a model with rather high vertical resolution: 20 model layers, each 0.5 m thick were used to represent the confining layer. SUB-CR model time steps correspond to the spacing of the symbols shown in Figure 5.2. Time steps of 4 and 6 days were used to cover the fast changes occurring in the first 10 days. Larger time steps were used for the subsequent simulated period. SUB-CR predicted subsidence tracks that of the other packages fairly closely. The slight underestimates of subsidence visible from 50 – 200 days were found to be caused by the still rather coarse time stepping (40 days) in the period from 10-50 days.
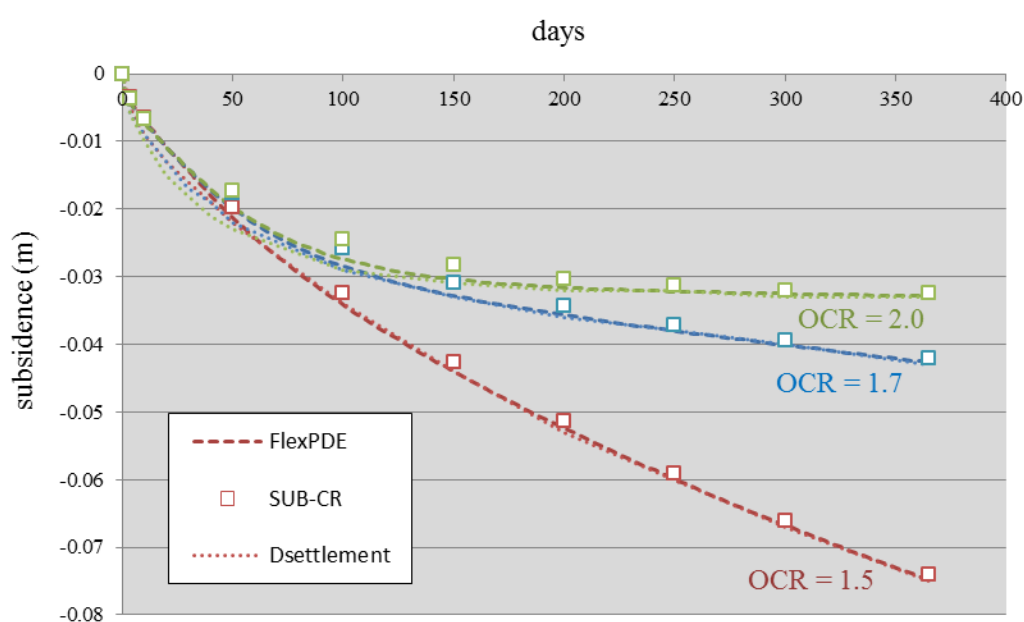

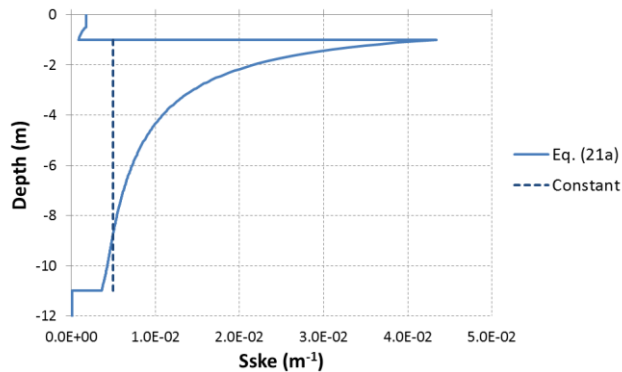*Figure continued on next page.*

Figure 5.2, Benchmark comparison for the 'small-strain' simulation with a drawdown of 1 m. Subsidence is shown for three values of OCR. For the SUB-CR results the symbol spacing reflects the time step size. SUB-CR results are for the NEN-Bjerrum model.

5.3.2 Large strain

Figure 5.3 displays results for simulations with large strains induced by a drawdown of 6 m. The simulated time here is extended to ten years. Local values of strain near the bottom of the confining layer (not shown in the figure) reach values of about 7% for *OCR*=1.5. Considering that the abc-model is the more accurate model (Den Haan, 1994a), results show that NEN-Bjerrum (linear strain) slightly overpredicts subsidence (~ 1-2%) in this case. Overprediction becomes less with smaller strain as demonstrated for the results for *OCR*=1.7. SUB-CR very closely reproduces the results of the other packages.
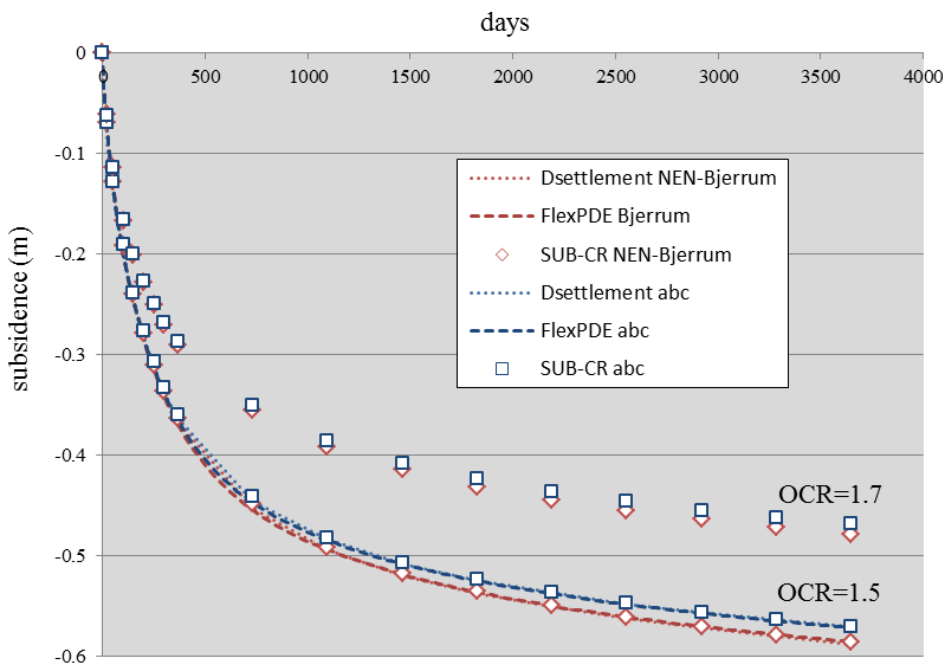

Figure 5.3, Benchmark comparison for a 'large-strain' simulation; drawdown of 6 m and OCR=1.5. SUB-CR results for OCR=1.7 show less subsidence and a smaller difference between the NEN-Bjerrum model and the abc-model.

5.4 Creep versus plastic (nominally 'no-creep') behavior

To illustrate the impact of creep, results are shown here for the previous simulations in which the secondary compression ratio C_α or secondary compression coefficient c is set to zero. As explained through Figure 3.3 and Figure 3.4, this approximates the behavior of the classical elastoplastic compression model in which creep rates are basically infinitely high up to a rigid yield boundary.

Figure 5.4 shows that impact of creep is very significant for the 'large strain' problem. Two key impacts can be discerned. One, creep enhances subsidence relative to that of an equivalent (same preconsolidation state) elastoplastic model. Two, creep causes a prolonged apparent hydrodynamic response. The large differences arise here because, in spite of the relatively large drawdown of 6 m, effective stress only marginally exceeds the preconsolidation stress for the adopted *OCR*=1.5 in the bottom half of the confining layer. In the top half of the layer effective stress stays below preconsolidation stress. The 'virgin' plastic strain, therefore, is very small in the elastoplastic model and the observed subsidence is dominated by elastic strain. For *OCR*=1.7 preconsolidation stress is nowhere exceeded and the subsidence is purely elastic. This not only explains the much smaller subsidence magnitude for the elastoplastic simulations, but also the short hydrodynamic delay. For the creep models, effective stress reaches similar levels. However, significant inelastic strain and subsidence does develop at these stress levels because creep strain rates are large close to, and non-negligible slightly below, the preconsolidation stress. Accumulation of inelastic strain and subsidence only ceases rapidly when effective stress in the confining layer decreases slightly.

This goes to show that the two types of models respond very differently when stresses reach levels close to or above the original preconsolidation stress. Obviously, responses are virtually identical when stresses stay significantly below the original preconsolidation stress and strain is within the elastic realm for both model types (this is demonstrated for the 'small-strain' case in the next paragraph). It should be noted that the differences are strongly emphasized in this illustrative example because of the chosen soft clay property, and that differences would be smaller for smaller C_α or *c*. Interestingly, Figure 5.4 also shows that responses become more comparable if different preconsolidation conditions are used in the two types of models. Compare, for instance, the OCR=1.7 creep model and the *OCR*=1.1 elastoplastic model.

Figure 5.5 provides a similar comparison for the 'small strain' simulations. The subsidence curves for the elastoplastic model are identical for all three *OCR* values because effective stress does not exceed the original preconsolidation stress anywhere in these simulations, and compression is purely elastic. Impact of creep is very minor for *OCR*=2.0. However, for *OCR*=1.5 the incurred creep strain after one year more than doubles that for the elastoplastic model. For the elastoplastic model this occurs when the preconsolidation stress virtually equals the initial effective stress (*OCR*=1.01).
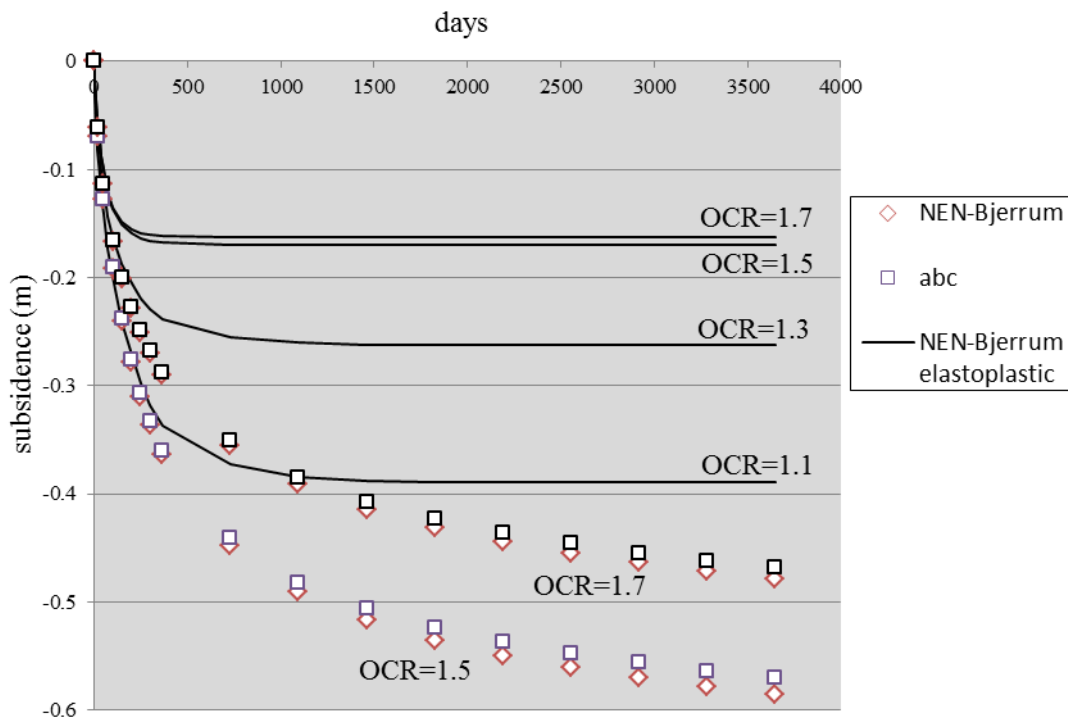
Figure 5.4 , Illustration of the impact of creep through comparison of the 'large-strain' simulations of Figure 5.3 with the equivalent (OCR=1.5 and 1.7) elastoplastic subsidence. Subsidence is also shown for elastoplastic models with the lower OCR values 1.1 and 1.3. Elastoplastic here refers to the inelastic strain being calculated as plastic ($C_\alpha \rightarrow 0$) rather than viscous strain.
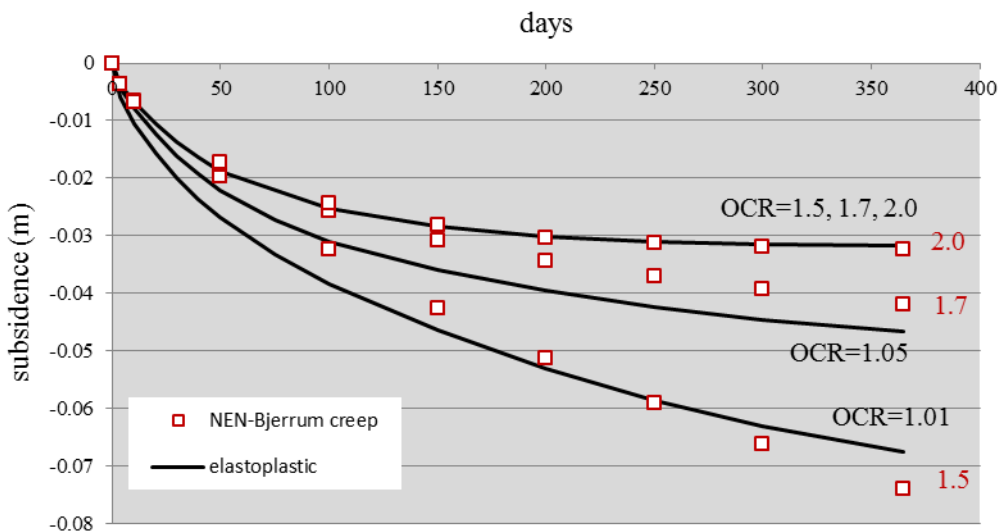

Figure 5.5, Illustration of the impact of creep through comparison of the 'small-strain' simulations of Figure 5.2 with the equivalent elastoplastic subsidence. The elastoplastic results apply to all three OCR values because preconsolidation stress is not exceeded.

5.5 Importance of sufficiently fine discretization

The previous sections already partly illustrated the impact of temporal discretization (time step size choice). However, sufficient (vertical) spatial discretization also is of crucial importance for confining layers.

Figures 5.6-5.8 separately show the 'small-strain' subsidence predictions of SUB-CR for OCR values of 1.5, 1.7 and 2.0, respectively, where the confining layer is discretized by a different number of model layers. The results clearly demonstrate that predictions become more accurate when the layer number increases. Using one model layer to represent the confining layer quantifies subsidence very poorly. Two or three model layers are needed to get reasonable results, but if great accuracy is required the confining layer needs to be represented by more model layers for this particular problem. In the simulations of the previous paragraphs, 20 layers were used because CPU time is no issue for these 1D simulations. In large regional applications, however, a compromise between accuracy and computation time may be warranted. No simple rules for sufficient discretization exist. In general it will depend on confining layer thickness and compression parameters. High-resolution discretization is particularly important when relatively high creep rates occur (here the OCR=1.5 case).
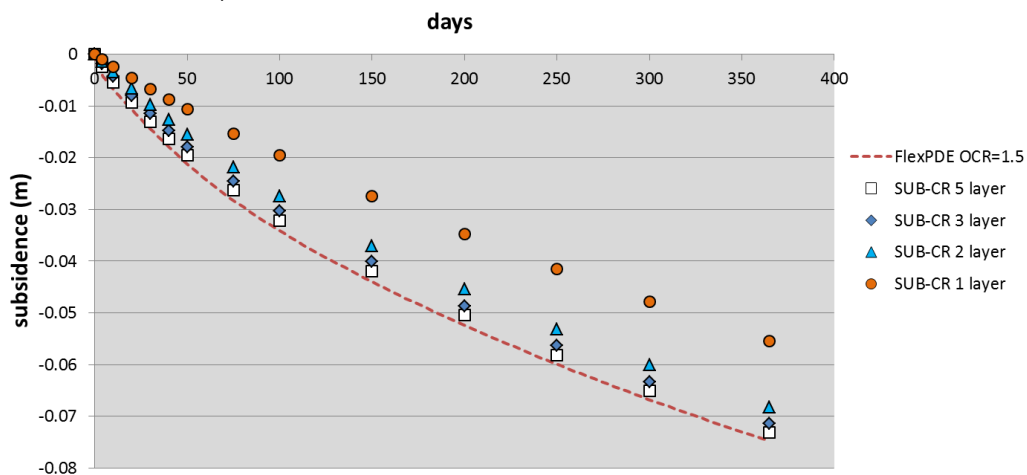

Figure 5.6, Impact of confining layer discretization for the 'small strain' simulations; OCR=1.5.
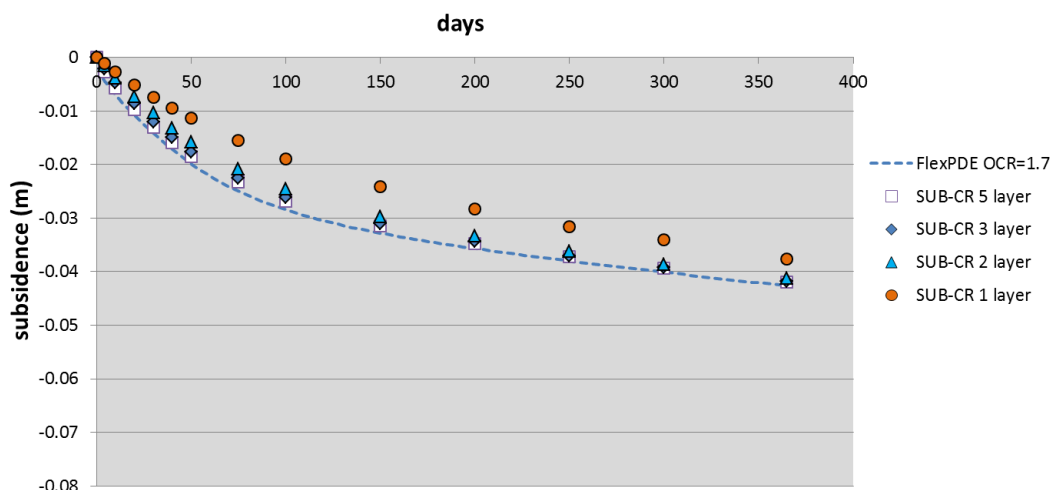

Figure 5.7, Impact of confining layer discretization for the 'small strain' simulations; OCR=1.7.
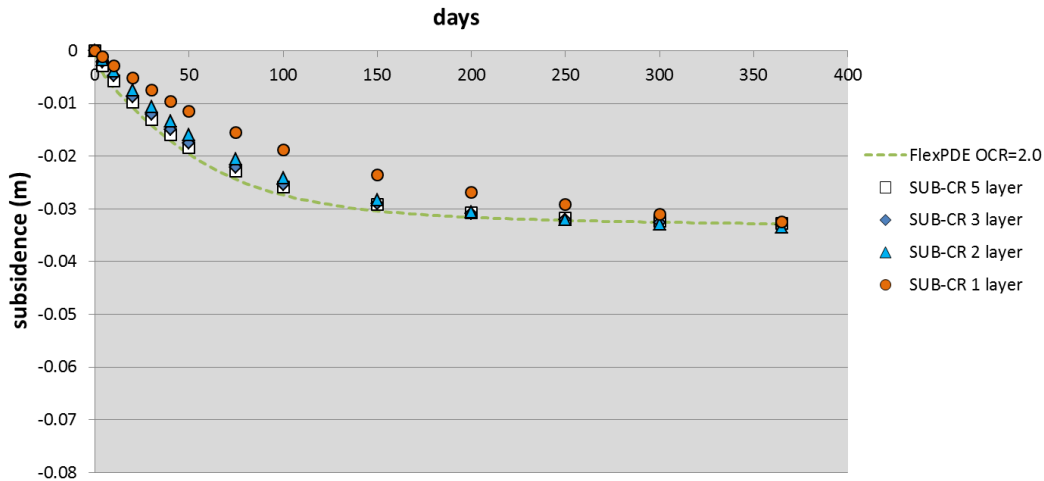
Figure 5.8, Impact of confining layer discretization for the 'small strain' simulations; OCR=2.0.

5.6 Example water budget

Figure 5.9 and Figure 5.10 display the cumulative water budget for the 'small strain' simulation with OCR=1.5 and for 5 model layers. The percent discrepancy reported in the .list file of the run is 0.00 for all time steps.
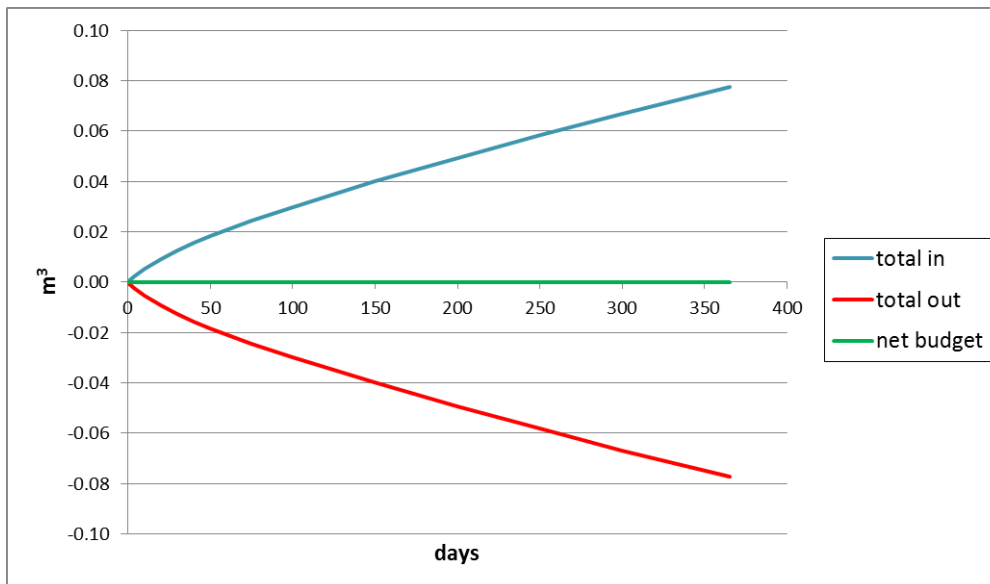

Figure 5.9, Graphical illustration of the cumulative water budget of the 'small strain' simulation with OCR=1.5 and for 5 model layers. This graph shows the net inflow and net outflow together with the net budget.

Figure 5.10 shows the non-zero budget components. The concave nature of the 'constant head in' component shows that inflow at the top of the domain progressively increases as the effect of the imposed drawdown below the clay layer propagates upward through the clay. Steady inflow is not established yet after one year. The 'storage in' component increases fast initially, but then levels off. This reflects the average elastic compression of the clay (and the

average drawdown) which should follow the same trend. The 'creep storage in' component shows an increase that is much more steady and persistent. This reflects the fact that once relatively high creep rates are induced by the increase in effective stress, these rates decline rather slowly after effective stress (and drawdown) stabilizes. After approximately 100 days, the average accumulated inelastic strain compression surpasses the average accumulated elastic strain. The very small 'storage out' component indicates that very minor elastic swelling also occurs within the model domain, coeval with the predominant elastic compression. This may be considered an artefact that is caused by the fact that the steady state head is calculated without creep. In the first transient time step, calculation creep is 'suddenly' turned on. This causes a slow increase of head in the clay that would continue until the creep compression is balanced by drainage. In the current model, the phase of head increase and swelling remains present for some time in the upper parts of the clay layer where the impact of the drawdown at the bottom boundary occurs with a delay.

Finally, inspection of the different components demonstrates that after one year (365 days), the cumulative inflow at the top of the model ('constant head in') constitutes but a small fraction of the cumulative outflow at the base ('head dep. out'). The cumulative outflow at the base at that time originates predominantly from storage within the clay that is 'squeezed' out out by elastic, but mostly by inelastic (creep) compression.
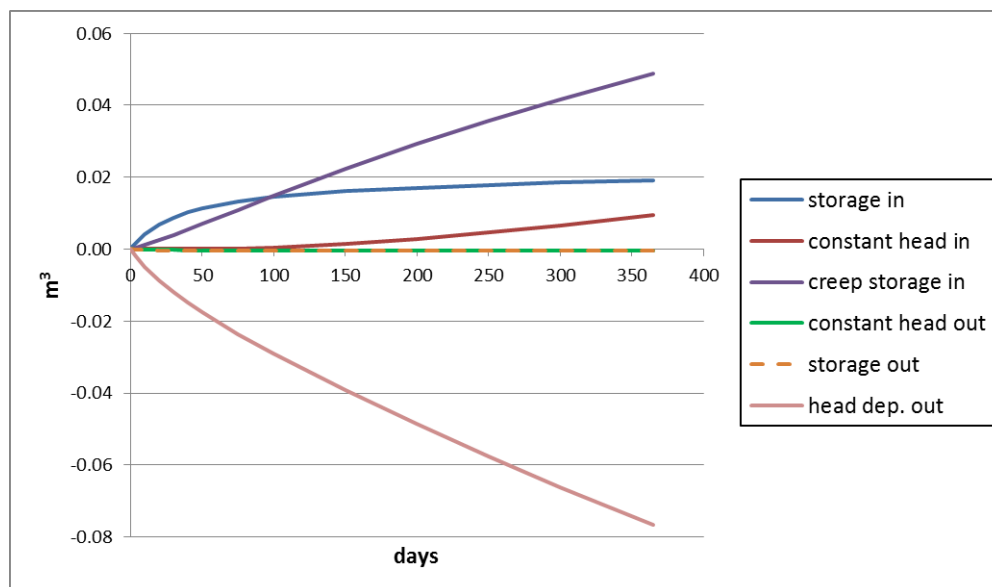

Figure 5.10, Graphical illustration of the cumulative water budget of the the 'small strain' simulation with OCR=1.5 and for 5 model layers. The graph shows the separate budget components. 'Storage in' and 'storage out' correspond to the elastic storage change associated with the specified S_{ske} values. 'Creep storage in' represents the inelastic storage change caused by creep. 'Constant head in' and 'constant head out' represent the flow at the top sand layer (see Figure 5.1). This layer is modeled using a constant head cell (CHD package). 'Head dep. out' corresponds to the flow the thin basal sand in the model. This layer is modeled with a general head boundary condition (GHB package).

6 References & literature

Bakr, M. (2015), Influence of Groundwater Management on Land Subsidence in Deltas, A Case Study of Jakarta (Indonesia), *Water Resour. Manag., 19*, 1541-1555, DOI 10.1007/s11269-014-0893-7.

Bear, J. (1972), Dynamics of fluids in porous media, American Elsevier Pub. Co.

Bjerrum, L. (1967), Engineering geology of Norwegian normally consolidated marine clays as related to settlements of buildings, *Géotechn., 17*(2), 81-118.

Buisman, K. (1936), Results of Long Duration Settlement Tests, Proceeding 1st International Conference on Soil Mechanics and Foundation Engineering, Cambridge, Massachusetts, *1*, 103-106.

Degago, S.A., G. Grimstad, H.P. Jostad, and S. Nordal (2013), Misconceptions about experimental substantiation of creep hypothesis A, *Proc. 18th Int. Conf. Soil Mech. and Found. Eng. Paris, 1*, 215-218.

Deltares (2011), D-Settlement version 16.1: Embankment Design and Soil Settlement Prediction; User Manual (https://content.oss.deltares.nl/delft3d/manuals/DSettlement_User_Manual.pdf).

Den Haan, E. J. (1994a), Vertical Compression of Soils, PhD. Dissertation, Technical University of Delft, 96 pp.

Den Haan, E.J. (1994b), Stress-independent parameters for primary and secondary compression, *Proc. 13th Int. Conf. Soil Mech. and Found. Eng. New Dehli*, *1*, 65-70.

Den Haan, E.J. (1996), A compression model for non-brittle soft clays and peat*, Géotechn. 1996 46:1, 1-16*, doi: 10.1680/geot.1996.46.1.1

Erkens, G., T. Bucx, R. Dam, G. de Lange, and J. Lambert (2015), Sinking Coastal Cities. *Proc. Int. Assoc. Hydrol. Sci. 372*: 189-198.

International Organization for Standardization (2004) Geotechnical investigation and testing – Laboratory testing of soil – Part 5: incremental loading oedometer test, ISO/TS 17892-5.

Galloway, D.L., Erkens, G., Kuniansky, E.L., and J.C. Rowland (2016) Preface: Land subsidence processes*, Hydrogeol. J. 24*, 547-550, doi: 10.1007/s10040-016-1386-y.

Galloway, D.L., and T.J. Burbey (2011), Review: Regional land subsidence accompanying groundwater extraction, *Hydrogeol. J. 19*, 1459-1486, doi: 10.1007/s10040-011-0775-5.

Gambolati, G., and R.A. Freeze (1973), Mathematical simulation of the subsidence of Venice: 1. Theory, *Water Resour. Res. 9*(3), 721–733.

Gambolati, G., and P. Teatini (2015), Geomechanics of subsurface water withdrawal and injection, *Water Resour. Res., 51*, 3922–3955, doi:10.1002/2014WR016841.

Giosan, L., J. Syvitski, S. Constantinescu, and J. Day (2014), Climate change: Protect the world's deltas. *Nature 516*, 31-33, doi:10.1038/516031a (2014).

Gray, H. (1936), Progress report on research on the consolidation of fine-grained soils, *Proc. 1st Int. Conf. Soil Mech. and Found. Eng. Cambridge, Mass., D14*, 138-141.

Harbaugh, A.W. (2005), MODFLOW-2005, the U.S. Geological Survey modular ground-water model -- the Ground-Water Flow Process: U.S. Geological Survey Techniques and Methods 6-A16.

Helm, D.C. (1986), COMPAC: a field-tested model to simulate and predict subsidence due to fluid withdrawal, *Austral. Geomech. Comp. Newslett., 10*, 18–20.

Helm, D.C. (1998), Poroviscosity, in *Land subsidence case studies and current research*, *Proceedings of the Dr. Joseph F. Poland Symposium on Land subsidence*, edited by Borchers, J.W., *Ass. of Eng. Geol. Spec. Pub. No. 8*, p. 395-405.

Hoffmann J., S.A. Leake, D.L. Galloway, and A.M. Wilson (2003), MODFLOW-2000 ground-water model—User guide to the subsidence and aquifer-system compaction (SUB) package, *US Geol. Surv. Open-File Rep 03–233* version 1.1.1.

Janbu, N. (1969), The resistance concept applied to deformations of soils, *Proc. 7th Int. Conf. Soil Mech. and Found. Eng., Mexico, Vol 1*, 191-196.

Jorgensen D.G. (1980), Relationships between basic soils-engineering equations and basic ground-water flow equations, *US Geol. Surv. Water Suppl. Pap., 2064*, http://pubs.er.usgs.gov/publication/wsp2064.

Leake S.A. (1990), Interbed storage changes and compaction in models of regional ground-water flow, *Water Resour. Res., 26* (9), 1939–1950.

Leake S.A., and D.E. Prudic (1991), Documentation of a computer program to simulate aquifer-system compaction using the modular finite-difference ground-water flow model, *US Geol. Surv. Tech. Water Resour. Invest., book 6*, chap. A2.

Leake S.A., and D.L. Galloway (2007), MODFLOW ground-water mode: user guide to the Subsidence and Aquifer-System Compaction Package (SUB-WT) for water-table aquifers, *USGS Tech. and Methods Rep. 6–A23.*

Leoni, M., M. Karstunen, and P.A. Vermeer (2008), Anisotropic creep model for soft soils, *Géotechn., 58(3)*, 215-226.

Leroueil, S. (2006), The isotache approach. Where are we 50 years after its development by Professor Suklje? (2006 Prof. Suklje's memorial lecture), *Proc. 13th Danube Eur. Conf. Geotech. Eng., Ljubljana 2*, 55–88.

Leroueil, S., and D.W. Hight (2003), Behaviour and properties of natural soils and soft rocks, in *Characterization and engineering properties of natural rocks*, *Vol. 1*, edited by Tan, T.S., et al., pp. 29-254.

Mesri, G. (1973), Coefficient of Secondary Compression, *J. Soil Mech. and Found. Division*, *99*, No. SM1, 123-137.

Mesri, G., and P.M. Godlewski (1977) Time- and stress- compressibility interrelationship. *J. Geotech. Eng. Div. ASCE 103*, GT5: 417-430.

Minderhoud, P.S.J., G. Erkens, V.H. Pham, V.T. Bui, L. Erban, H. Kooi, and E. Stouthamer (2017), Impacts of 25 years of groundwater extraction on subsidence in the Mekong delta, Vietnam, *Environ. Res. Lett. 12*, 064006, doi:10.1088/1748-9326/aa7146

Mitchell J.K. (1993), Fundamentals of soil behaviour, 2nd edition, John Wiley & Sons, Inc, New York, 437 pp.

Neuzil, C.E. (2003), Hydromechanical coupling in geologic processes, Hydrogeol. J. 11, 41-83.

NNI (2012), NEN9997-1+C1: Geotechnical design of structures; Part 1: General rules (in Dutch). Nederlands Normalisatie Instituut (Dutch Normalization Institute), 306 p.

Olsson, M. (2010), CalcuVlating long-term settlement in soft clays – with special focus on the Gothenburg region, *Swedish Geotech. Inst. Rep. 74*, Linköping, Sweden, 117 p.

Poland J.F., and G.H. Davis (1969), Land subsidence due to withdrawal of fluids, *Rev. Eng. Geol, 2*, 187–269.

Poland, J.F., B.E. Lofgren, R.L. Ireland, and R.G. Pugh (1975), Land subsidence in the San Joaquin Valley, California, as of 1972, *U.S. Geol. Surv. Prof. Pap. 437-H*, 78 p.

SBRCURnet (2005), CUR-recommendation 101: Execution and interpretation compression test (in Dutch) 58 pp (http://www.sbrcurnet.nl/producten/curaanbevelingen/aanbeveling-101).

Schiermeier, Q. (2014), Floods: Holding back the tide. *Nature 508*, 164-166, doi:10.1038/508164a

Schmidt, C. (2015), Alarm over a sinking delta. *Science 348*, 845-846, doi:10.1126/science.348.6237.845

Šuklje, L. (1957), The analysis of the consolidation process by the isotaches method. *Proc. 4th Int. Conf. Soil Mech. and Found. Eng. London, Vol. 1*, 200-206.

Syvitski, J. P. M. et al. (2009), Sinking deltas due to human activities. *Nature Geosci. 2*, 681-686.

Szavits-Nossan, V. (1988), Intrinsic time behavior of cohesive soils during consolidation, PhD thesis, Dept. of Civil, Environmental and Architectural Engineering, University of Colorado, Boulder.

Taylor, D.W., and W. A. Merchant (1940), A theory of clay consolidation accounting for secondary compression, *J. of Math. and Phys., 19*, 167-185.

Taylor, D. W. (1942), Research on consolidation of clays, *Massachusetts Institute of Technology - Department of Civil and Sanitary Engineering - Serial*, 147 p.

Terzaghi, K. (1925), *Settlement and consolidation of clay*, McGraw-Hill, New York, pp. 874–878   .

Wilson, J.D., and R.L. Naff (2004) The U.S. Geological Survey modular ground-water model – GMG linear equations solver package documentation: *US Geol. Surv. Open-File Rep 2004-1261.*

7 Appendixes

A Temporal integration of the compression models

A.1 NEN-Bjerrum model

Coupled with the groundwater flow model, the strain needs to be updated for each model time step. This procedure is implemented as follows.

A time step is represented by $\Delta t = t^n - t^{n-1}$ where the superscript indicates the time level. The elastic strain increment is given by (see also Eq 10a)

$$\Delta \varepsilon_e = RR \log \left(\frac{\sigma'^{(n)}}{\sigma'^{(n-1)}} \right) \tag{A.1}$$

The creep increment (based on Eq. 8) is calculated from

$$\Delta \varepsilon_{cr} = C_\alpha \log \left(\frac{\tau^n}{\tau^*} \right); \qquad \tau^n = \tau^* + \Delta t; \qquad \tau^* = \tau^{n-1} \left(\frac{\sigma'^{(n-1)}}{\sigma'^{(n)}} \right)^{\frac{CR-RR}{C_\alpha}} \tag{A.2}$$

where τ^* is the intrinsic time that can be inferred from the stress-strain diagram (Figure 3.3) at the end of the time step if elastic deformation is considered only. Note that during integration intrinsic time is continually updated. To start calculation the following parameters need to be specified: the three compression parameters, the initial effective stress $\sigma'^{(0)} = \sigma'_o$, and the initial intrinsic time τ_o. The latter is not specified directly, but calculated from either the initial overconsolidation ratio $OCR^{(0)}$, or the initial preconsolidation stress $\sigma'^{(0)}_p$ using the general relationships

$$\tau = \tau_{ref} OCR^{\frac{CR-RR}{C_\alpha}}; \qquad OCR = \sigma'_p / \sigma' \tag{A.3}$$

This relationship also allows simple determination of $OCR^{(n)}$, and $\sigma'^{(n)}_p$ from the momentary τ^n during the modeling.

For $C_\alpha < 10^{-4}$, evaluation of τ^* in Eq. (A.2) can be problematic as the power $(CR-RR)/C_\alpha$ tends to be very large. Under those circumstances, which approximate an elastic-plastic type compression behavior, the package resorts to a different integration method to calculate the creep strain increment. Here the momentary preconsolidation stress is explicitly updated at the end of a time step. That is, if $\sigma'^{(n)} > \sigma'^{(n-1)}_p$, then $\sigma'^{(n)}_p = \sigma'^{(n)}$, else $\sigma'^{(n)}_p = \sigma'^{(n-1)}_p$. The creep strain increment follows from Eq. (10b) by neglecting the second term.

$$\Delta\varepsilon_{cr} = (CR - RR)\log\left(\frac{\sigma'^{(n)}}{\sigma'^{(n-1)}_p}\right); \qquad\qquad \sigma'^{(n)} > \sigma'^{(n-1)}_p \qquad\qquad (A.4a)$$

$$\Delta\varepsilon_{cr} = 0; \qquad\qquad \sigma'^{(n)} \leq \sigma'^{(n-1)}_p \qquad\qquad (A.4b)$$

A.2 abc-model

Incremental strain updates are calculated using (see Eqs 14 and 12))

$$\Delta\varepsilon_e^H = a\ln\left(\frac{\sigma'^{(n)}}{\sigma'^{(n-1)}}\right) \qquad\qquad (A.5)$$

$$\Delta\varepsilon_{cr}^H = c\ln\left(\frac{\tau^n}{\tau^*}\right); \qquad \tau^n = \tau^* + \Delta t; \qquad \tau^* = \tau^{n-1}\left(\frac{\sigma'^{(n-1)}}{\sigma'^{(n)}}\right)^{\frac{b-a}{c}} \qquad (A.6)$$

$$\tau = \tau_{ref}OCR^{\frac{b-a}{c}}; \qquad OCR = \sigma'_p/\sigma' \qquad\qquad (A.7)$$

When the elastoplastic limit is approached (quantified by $c \leq 10^{-4}$) calculation uses:

$$\Delta\varepsilon_{cr}^H = (b-a)\ln\left(\frac{\sigma'^{(n)}}{\sigma'^{(n-1)}_p}\right); \qquad\qquad \sigma'^{(n)} > \sigma'^{(n-1)}_p \qquad\qquad (A.8a)$$

$$\Delta\varepsilon_{cr}^H = 0; \qquad\qquad \sigma'^{(n)} \leq \sigma'^{(n-1)}_p \qquad\qquad (A.8b)$$

B Derivation of the groundwater flow equation and elucidation of underlying assumptions

Here, first the groundwater flow equation that includes the coupling with the abc-model is derived. The derivation follows Bear (1972) and Den Haan (1994a). Only limited assumptions are made in the derivation and the resulting partial differential equation, therefore, is in a rather fundamental form. Subsequently, it is shown how this equation is simplified to the form employed in the SUB-CR package (Eqs 16-17), and the assumptions involved are listed and discussed. Finally, the derivation for the NEN-Bjerrum model – differences relative to the abc-model are minor - is provided. The derivation for the abc-model is given first because it links 'more naturally' with the mass balance equation of Bear (1972).

B.1 abc-model

B.1.1 Derivation

Bear (1972) demonstrated that for a homogeneous incompressible fluid, mass conservation in a consolidating, fully saturated medium is given by (combining his Eqs 6.3.20 and 6.2.22)

$$\frac{\partial q_{r,x}}{\partial x} + \frac{\partial q_{r,y}}{\partial y} + \frac{\partial q_{r,z}}{\partial z} = \frac{D\varepsilon^H}{Dt} \tag{B.1}$$

The subscript 'r' refers to specific discharge relative to the rock/solid frame, and D/Dt denotes the substantial or material derivative (relative to the moving solids). In Bear's notation the material derivative is written as d_s/dt. Note that in Eq. (B.1) strain is taken positive for compression. In view of the fact that Darcy's law gives the specific discharge with respect to the moving solids the subscript 'r' is further dropped (Bear, 1972), and substitution of the expressions for the discharge components yields

$$\frac{\partial}{\partial x}\left(-K_x \frac{\partial h}{\partial x}\right) + \frac{\partial}{\partial y}\left(-K_y \frac{\partial h}{\partial y}\right) + \frac{\partial}{\partial z}\left(-K_z \frac{\partial h}{\partial z}\right) = \frac{D\varepsilon^H}{Dt} \tag{B.2}$$

Because of the material derivative in Eq. (B.2), it is convenient to use the Lagrangian method and label the moving solids by their initial vertical coordinate (Lagrangian or material coordinate), $\zeta = z(t=0)$, as shown in Figure B.1.
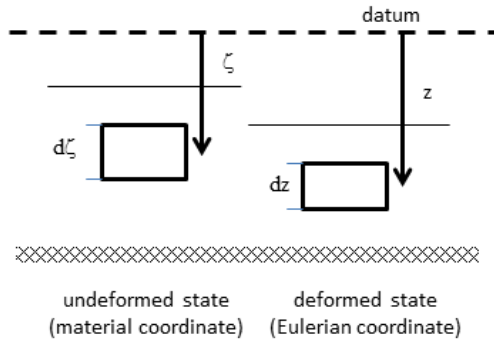
Figure B.1, Graphical representation of the Lagrangian/material (linked to the solids) and Eulerian coordinates and spatial increments used in the derivation. Positive coordinates are taken upward to facilitate use of head as a dependent variable.

The 'true' (Eulerian) vertical position at any time due to compaction is then given by $z = z(\zeta, t)$. Material coordinates are also required for the horizontal coordinates $\xi = x(t = 0)$ and $\psi = y(t = 0)$, where $\xi = x$ and $\psi = y$ for all time due to the assumption that compression acts vertically only. We refrain from formally implementing these material coordinates to avoid very lengthy expressions with all cross-terms of the transformation and directly apply

$$\frac{\partial}{\partial \xi} = \frac{\partial}{\partial x} \quad \text{and} \quad \frac{\partial}{\partial \psi} = \frac{\partial}{\partial y} \tag{B.3}$$

This basically implies that changes in the gradient (of head) along material layers due to tilting by differential subsidence are neglected (this is compatible with MODFLOW in which the impact of the inclination of model layers on 'along-layer derivatives' (row- or column direction) is neglected).

As the compressibility of the solid phase can generally be neglected,

$$dz = \frac{v}{v_o} d\zeta \tag{B.4}$$

where v denotes specific volume (total volume per volume of solids) and v_o the initial specific volume. The strain rate is partitioned into the elastic and creep strain rate

$$\frac{D\varepsilon^H}{Dt} = \frac{D\varepsilon_e^H}{Dt} + \frac{D\varepsilon_{cr}^H}{Dt} \tag{B.5}$$

For the abc-model

$$\varepsilon_e^H = a \ln \frac{\sigma'}{\sigma_o'} \quad \Rightarrow \quad \frac{D\varepsilon_e^H}{Dt} = \frac{a}{\sigma'} \frac{D\sigma'}{Dt} \tag{B.6}$$

and

$$\frac{D\varepsilon_{cr}^{H}}{Dt} = \frac{c}{\tau}$$

(B.7)

where $\sigma^{'}$ is effective stress, and τ intrinsic time, both evaluated for material coordinates. Combining Eqs (B.2-B.7) yields

$$\frac{\partial}{\partial x}\left(-K_x\frac{\partial h}{\partial x}\right) + \frac{\partial}{\partial y}\left(-K_y\frac{\partial h}{\partial y}\right) + \frac{v_o}{v}\frac{\partial}{\partial \zeta}\left(-K_z\frac{v_o}{v}\frac{\partial h}{\partial \zeta}\right) = \frac{a}{\sigma^{'}}\frac{D\sigma^{'}}{Dt} + \frac{c}{\tau}$$

(B.8)

Finally, effective stress change is written in terms of head change using

$$D\sigma^{'} = D(\sigma - p) = D\sigma - Dp = D\sigma - D\gamma_w(h - z) = D\sigma - \gamma_w Dh + \gamma_w Dz$$

(B.9)

where σ, p and γ_w are geostatic stress, pore pressure and the specific weight of water, respectively. Substitution of Eq. (B.9) in (B.8) and multiplying by -1 yields

$$\frac{\partial}{\partial x}\left(K_x\frac{\partial h}{\partial x}\right) + \frac{\partial}{\partial y}\left(K_y\frac{\partial h}{\partial y}\right) + \frac{v_o}{v}\frac{\partial}{\partial \zeta}\left(K_z\frac{v_o}{v}\frac{\partial h}{\partial \zeta}\right) =$$

$$\gamma_w\frac{a}{\sigma^{'}}\frac{Dh}{Dt} - \frac{a}{\sigma^{'}}\frac{D\sigma}{Dt} - \gamma_w\frac{a}{\sigma^{'}}\frac{Dz}{Dt} - \frac{c}{\tau}$$

(B.10)

As shown by Eq. (B.3) the spatial derivatives in the first two terms approximate material derivatives and may, therefore, be interpreted as such without change of notation.

B1.2 Comparison with the conventional MODFLOW equation and elucidation of terms

The groundwater equation solved in MODFLOW is generally reported to be of the form

$$\frac{\partial}{\partial x}\left(K_x\frac{\partial h}{\partial x}\right) + \frac{\partial}{\partial y}\left(K_y\frac{\partial h}{\partial y}\right) + \frac{\partial}{\partial z}\left(K_z\frac{\partial h}{\partial z}\right) = S_s\frac{\partial h}{\partial t} - Q$$

(B.11)

where S_s is specific storage, and Q contains sources, usually water injection or withdrawal by pumping or by various types of boundary conditions. All properties and dependent variables ($K_x, K_y, K_z, S_s Q, h$) are linked to fixed space x, y, z, as well as to the solids of the porous medium (parts of aquifer or confining units that are represented by MODFLOW finite difference cells). To facilitate comparison with Eq. (B.10), the MODFLOW equation can, therefore, also be presented in terms of material coordinates as:

$$\frac{\partial}{\partial x}\left(K_x\frac{\partial h}{\partial x}\right) + \frac{\partial}{\partial y}\left(K_y\frac{\partial h}{\partial y}\right) + \frac{\partial}{\partial \zeta}\left(K_z\frac{\partial h}{\partial \zeta}\right) = S_s\frac{Dh}{Dt} - Q$$

(B.12)

Comparison with Eq. (B.10) shows that for the compacting and subsiding system

$$S_s = \gamma_w \frac{a}{\sigma'} \tag{B.13a}$$

$$Q = \frac{a}{\sigma'} \frac{D\sigma}{Dt} + \gamma_w \frac{a}{\sigma'} \frac{Dz}{Dt} + \frac{c}{\tau} \tag{B.13b}$$

Moreover, for the compacting and subsiding system each vertical derivative in the material coordinate should be multiplied by v_o / v.

The following observations can be made regarding Eq. (B.10):

1   Specific storage is controlled by elastic strain only Eq. (B.13a). No other (inelastic) forms of specific storage are involved. Specific storage is proportional to the reciprocal of effective stress. Additional storage associated with water compressibility would appear if introduced in Eq. (B.1) (Bear, 1972).

2   Three source terms can be distinguished in Eq. (B.13b):
The first term represents the effect of changes in overburden weight (geostatic stress).
The second term accounts for the effect of the change in vertical position of the sediment, and hence, of the 'elevation head' of the groundwater. The latter is relative to the absolute datum for head, elevation and subsidence measurements; for instance a constant sea level. If tectonic movements are negligible, the second source term corresponds to subsidence due to compression of underlying units. It is important to note that if this term is included in modeling, it should also apply to aquifer units that are not susceptible to compression. Inspection of Eq. (B.10) shows that, in the absence of other contributions, subsidence causes a corresponding negative change (decrease) of head directly proportional to the subsidence, as it should.
The third term (denoted by Q_{creep} in Eq. (16) in the main text) represents the effect of creep strain (this compresses the pore water). Elastic strain does not act as a source term; it is 'passively' involved via its impact on storage.

3   Vertical gradients are enhanced by the ratio of original and deformed specific volume. This is accounts for the fact that compression reduces vertical distances in the porous sediment framework.

B.1.3 Simplifications/assumptions

The groundwater flow equation employed in the present version of the SUB-CR package is provided by Eq. (16) in the main body of the paper. Comparison with Eq. (B.10) demonstrates that the following assumptions are implied:

Firstly, changes in vertical gradients of hydraulic head and hydraulic conductivity caused by compression of sediments are assumed to have a negligible effect on the temporal evolution of hydraulic head (as is the case in other subsidence packages as SUB and SUB-WT).

Secondly, the net effect of changes in geostatic stress and changes in vertical position (sum of the first and second 'source terms' in Eq. (B.13b)) due to sediment compression is assumed to be zero. This is a very reasonable assumption if the water expelled from underlying compacting sediments would move upward and remain in the same vertical column of sediments as depicted in Figure B.2.
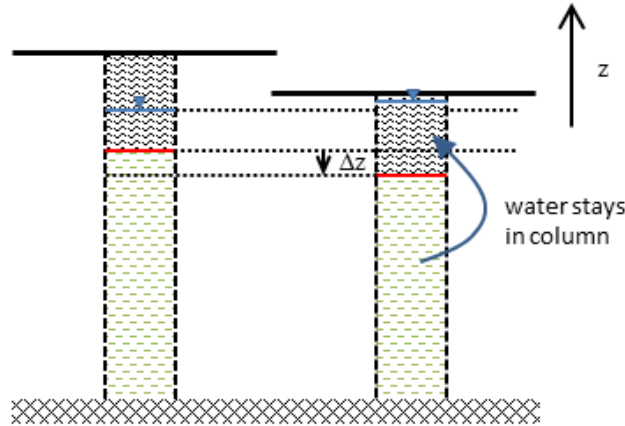
Figure B.2,   Graphical representation of conditions under which the combination of the first and second source term in Eq. (B.13b) is negligible, as assumed in the present version 1.0 of SUB-CR. The deformed vertical coordinate (Fig. B.1) is used in the figure.

While this can be approximately the case if a laterally extensive surface load drives the consolidation (for instance sedimentation over an extensive area), for subsidence induced by groundwater extraction the change in vertical position is not generally compensated by an equivalent increase in geostatic stress. That is, hydraulic head would tend to decrease in areas of sediment compression and subsidence, inducing a compensating flow of groundwater towards those loci of subsidence trying to restore steady state conditions when subsidence abates and, ultimately, a rising of the water table relative to the land surface (and potential ponding in extreme conditions). In the present version of SUB-CR these processes are neglected (as is the case in other subsidence packages as SUB and SUB-WT).

B.2 NEN-Bjerrum model

B.2.1 Derivation

Symbols used in this section are the same as those defined in section B.1. Using $\varepsilon^H = -\ln(1-\varepsilon)$, Bear's mass conservation equation (B.2) in terms of linear (or Cauchy) strain becomes

$$\frac{\partial}{\partial x}\left(-K_x\frac{\partial h}{\partial x}\right)+\frac{\partial}{\partial y}\left(-K_y\frac{\partial h}{\partial y}\right)+\frac{\partial}{\partial z}\left(-K_z\frac{\partial h}{\partial z}\right)=\frac{1}{1-\varepsilon}\frac{D\varepsilon}{Dt} \tag{B.14}$$

Recognizing that $1-\varepsilon = v/v_o$, Eq. (B.14) can also be written as

$$\frac{\partial}{\partial x}\left(-K_x\frac{\partial h}{\partial x}\right)+\frac{\partial}{\partial y}\left(-K_y\frac{\partial h}{\partial y}\right)+\frac{\partial}{\partial z}\left(-K_z\frac{\partial h}{\partial z}\right)=\frac{v_o}{v}\frac{D\varepsilon}{Dt} \tag{B.15}$$

The rate of linear strain is again partitioned into the elastic and creep strain rate

$$\frac{D\varepsilon}{Dt} = \frac{D\varepsilon_e}{Dt} + \frac{D\varepsilon_{cr}}{Dt} \tag{B.16}$$

where, for NEN-Bjerrum,

$$\varepsilon_e = RR \log \frac{\sigma'}{\sigma_o'} \quad \Rightarrow \quad \frac{D\varepsilon_e}{Dt} = \frac{RR}{\ln(10)\sigma'} \frac{D\sigma'}{Dt} \tag{B.17}$$

and

$$\frac{D\varepsilon_{cr}}{Dt} = \frac{C_\alpha}{\ln(10)\tau} \tag{B.18}$$

Combining Eqs (B.15-B.18) yields

$$\frac{\partial}{\partial x}\left(-K_x \frac{\partial h}{\partial x}\right) + \frac{\partial}{\partial y}\left(-K_y \frac{\partial h}{\partial y}\right) + \frac{\partial}{\partial z}\left(-K_z \frac{\partial h}{\partial z}\right) = \frac{v_o}{v}\left[\frac{RR}{\ln(10)\sigma'}\frac{D\sigma'}{Dt} + \frac{C_\alpha}{\ln(10)\tau}\right] \tag{B.19a}$$

And with Eq. (B.4) this is written as

$$\frac{\partial}{\partial x}\left(-K_x \frac{\partial h}{\partial x}\right) + \frac{\partial}{\partial y}\left(-K_y \frac{\partial h}{\partial y}\right) + \frac{v_o}{v}\frac{\partial}{\partial \zeta}\left(-K_z \frac{v_o}{v}\frac{\partial h}{\partial \zeta}\right) =$$
$$\frac{v_o}{v}\left[\frac{RR}{\ln(10)\sigma'}\frac{D\sigma'}{Dt} + \frac{C_\alpha}{\ln(10)\tau}\right] \tag{B.19b}$$

Finally, combining Eqs (B.9) and (B.19b) yields

$$\frac{\partial}{\partial x}\left(K_x \frac{\partial h}{\partial x}\right) + \frac{\partial}{\partial y}\left(K_y \frac{\partial h}{\partial y}\right) + \frac{v_o}{v}\frac{\partial}{\partial \zeta}\left(K_z \frac{v_o}{v}\frac{\partial h}{\partial \zeta}\right) =$$
$$\frac{1}{\ln(10)}\frac{v_o}{v}\left[\gamma_w \frac{RR}{\sigma'}\frac{Dh}{Dt} - \frac{RR}{\sigma'}\frac{D\sigma}{Dt} - \gamma_w \frac{RR}{\sigma'}\frac{Dz}{Dt} - \frac{C_\alpha}{\tau}\right] \tag{B.20}$$

B.2.2. Comparison with the conventional MODFLOW equation and clarification of terms

Specific storage and source terms are:

$$S_s = \gamma_w \frac{v_o}{v} \frac{RR}{\ln(10)\sigma'} \tag{B.21a}$$

$$Q_{geostatic} = \frac{v_o}{v} \frac{RR}{\ln(10)\sigma'} \frac{D\sigma}{Dt} \tag{B.21b}$$

$$Q_{subsidence} = \gamma_w \frac{v_o}{v} \frac{RR}{\ln(10)\sigma'} \frac{Dz}{Dt} \tag{B.21c}$$

$$Q_{creep} = \frac{v_o}{v} \frac{C_\alpha}{\ln(10)\tau} \tag{B.21d}$$

And vertical material derivatives are multiplied by v_o / v in the same way as for the abc-model.

B.2.3 Simplifications/assumptions

Comparison of Eq. (16) in the main text with Eq. (B.20) demonstrates that the following assumptions are implied:
1 Changes in vertical gradients of hydraulic head and hydraulic conductivity caused by compression of sediments are assumed to have a negligible effect on the temporal evolution of hydraulic head.
2 The net effect of changes in geostatic stress and changes in vertical position (sum of the first and second 'source terms' (Eqs B.21b; B.21c)) due to sediment compression is assumed to be zero.
3 The factor v_o / v in the creep source term (Eq. B.21d) and in the elastic specific storage (Eq. B.21a) is neglected.